AD-A118 314 UTAH STATE UNIV LOGAN F/G 20/6
SPECTROSCOPIC STUDY OF SMALL ABSORPTIONS IN OPTICAL COATINGS.(U)
JUL 82 W N HANSEN F29601-79-C-0064
UNCLASSIFIED AFWL-TR-81-139 NL

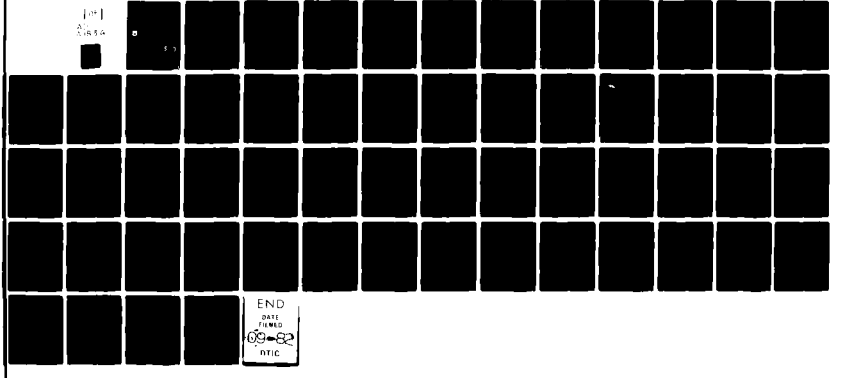

END
DATE FILMED
09-82
DTIC

AFWL-TR-
81-139

(2)

SPECTROSCOPIC STUDY OF SMALL ABSORPTIONS IN OPTICAL COATINGS

Wilford N. Hansen

Utah State University
Logan, UT 84322

July 1982

Final Report

Approved for public release; distribution unlimited.

AIR FORCE WEAPONS LABORATORY
Air Force Systems Command
Kirtland Air Force Base, NM 87117

This final report was prepared by Utah State University, Logan, Utah under Contract F29601-79-C-0064, Job Order 317J0834 with the Air Force Weapons Laboratory, Kirtland Air Force Base, New Mexico. Dr Alan F. Stewart (ARAO) was the Laboratory Project Officer-in-Charge.

When Government drawings, specifications, or other data are used for any purpose other than in connection with a definitely Government-related procurement, the United States Government incurs no responsibility or any obligation whatsoever. The fact that the Government may have formulated or in any way supplied the said drawings, specifications, or other data, is not to be regarded by implication, or otherwise in any manner construed, as licensing the holder, or any other person or corporation; or as conveying any rights or permission to manufacture, use, or sell any patented invention that may in any way be related thereto.

This report has been authored by a contractor of the United States Government. Accordingly, the United States Government retains a nonexclusive, royalty-free license to publish or reproduce the material contained herein, or allow others to do so, for the United States Government purposes.

The Public Affairs Office has reviewed this report, and it is releasable to the National Technical Information Service, where it will be available to the general public, including foreign nationals.

If your address has changed, if you wish to be removed from our mailing list, or if your organization no longer employs the addressee, please notify AFWL/ARAO, Kirtland AFB, NM 87117, to help us maintain a current mailing list.

Alan F. Stewart

ALAN F. STEWART
Project Officer

FOR THE COMMANDER

James W Mayo III

JAMES W. MAYO, III
Lt Colonel, USAF
Chief, Adv Resonator/Optics Branch

David W. Seegmiller

DAVID W. SEEGMILLER
Colonel, USAF
Chief, Adv Laser Technology Division

DO NOT RETURN COPIES OF THIS REPORT UNLESS CONTRACTUAL OBLIGATIONS OR NOTICE ON A SPECIFIC DOCUMENT REQUIRES THAT IT BE RETURNED.

UNCLASSIFIED

SECURITY CLASSIFICATION OF THIS PAGE *(When Data Entered)*

REPORT DOCUMENTATION PAGE		READ INSTRUCTIONS BEFORE COMPLETING FORM
1. REPORT NUMBER AFWL-TR-81-139	2. GOVT ACCESSION NO. AD-A118 314	3. RECIPIENT'S CATALOG NUMBER
4. TITLE *(and Subtitle)* SPECTROSCOPIC STUDY OF SMALL ABSORPTIONS IN OPTICAL COATINGS		5. TYPE OF REPORT & PERIOD COVERED Final Report 6. PERFORMING ORG. REPORT NUMBER
7. AUTHOR(s) Wilford N. Hansen		8. CONTRACT OR GRANT NUMBER(s) F29601-79-C-0064
9. PERFORMING ORGANIZATION NAME AND ADDRESS Utah State University Logan, Utah 84322		10. PROGRAM ELEMENT, PROJECT, TASK AREA & WORK UNIT NUMBERS 63605F/317J0834
11. CONTROLLING OFFICE NAME AND ADDRESS Air Force Weapons Laboratory (ARAO) Kirtland Air Force Base, New Mexico 87117		12. REPORT DATE July 1982 13. NUMBER OF PAGES 58
14. MONITORING AGENCY NAME & ADDRESS*(if different from Controlling Office)*		15. SECURITY CLASS. *(of this report)* UNCLASSIFIED 15a. DECLASSIFICATION/DOWNGRADING SCHEDULE

16. DISTRIBUTION STATEMENT *(of this Report)*

Approved for public release; distribution unlimited.

17. DISTRIBUTION STATEMENT *(of the abstract entered in Block 20, if different from Report)*

18. SUPPLEMENTARY NOTES

19. KEY WORDS *(Continue on reverse side if necessary and identify by block number)*

Optical Coatings
Thin Film Characterization
Reflection Spectroscopy of Thin Films
Laser Optical Coatings
Thorium Fluoride
Zinc Selenide
Optical Constants
Liquids
Lorentz Local Field Theory

20. ABSTRACT *(Continue on reverse side if necessary and identify by block number)*

This report concerns research performed by the Utah State University surface physics group for the Air Force Weapons Laboratory (AFWL), Kirtland Air Force Base, New Mexico. It is a supplement to AFWL-TR-79-197. It reports the continued study of thorium fluoride (ThF_4) as an optical coating, showing that the moisture found in the ThF_4 films probably originated from the preparation itself, and that ThF_4 may not degrade by moisture absorption from the atmosphere as rapidly as previously thought. Further advances are reported in the

(Continued)

DD FORM 1 JAN 73 1473 EDITION OF 1 NOV 65 IS OBSOLETE

UNCLASSIFIED

SECURITY CLASSIFICATION OF THIS PAGE *(When Data Entered)*

Block No. 20 (Continued)

characterization procedures themselves, including computer methods for data handling. New procedures were instituted for determining the optical constants of liquids. To test the procedures, the optical constants of liquid water were determined and compared with values found in literature. The procedures used are reported. A sample of Si_3N_4 film on germanium was analyzed spectroscopically. The dominant feature was a large infrared band revealing the presence of large amounts of silicon hydride. Finally, new procedures are reported for determining impurity concentrations in optical thin films which takes into account the local electromagnetic field strength seen by an impurity in a known optical material as matrix.

PREFACE

This report is a supplement to AFWL-TR-79-197 prepared under Contract F29601-79-C-0064, summarizing additional work performed under an extension of that contract through May 30, 1981.

The main efforts of the program are the characterization of small impurity absorptions in a group of optical coatings and, especially for the work reported here, the development of sensitive techniques to identify, locate and quantify impurities.

CONTENTS

ILLUSTRATIONS

I. INTRODUCTION

As stated in AFWL-TR-79-197, the approach of the present optical study is based upon procedures given in the recent paper, "Reflection Spectroscopy of Optical Coatings" (Ref. 1) and the theoretical paper, "Electric Fields Produced by the Propagation of the Plane Coherent Electromagnetic Radiation in a Stratified Medium" (Ref. 2). While the approach is applicable to any wavelength region, the work documented in this report was in the 2.5- to 50- μm infrared (IR) region, with emphasis on the important laser wavelength regions.

The general accomplishments of the program are categorized as in AFWL-TR-79-197, viz.:

1. NEW SENSITIVE METHODS AND PROCEDURES

New sensitive methods and procedures have been developed and used to characterize small absorptions in optical coatings, both qualitatively and quantitatively. Qualitative analysis seeks to identify the source of the absorption, e.g., the actual chemical species involved. Quantitative analysis emphasizes the extent of the absorption as a function of wavelength and the amount of the species involved.

2. OPTICAL LAYERS AND MULTILAYERS

Various optical layers and multilayers have been examined in detail for absorbing impurities. The offending species have been identified, located, and amounts determined. The coatings were designed to represent typical state-of-the-art products. All coatings examined showed absorbing impurities in important laser wavelength regions.

3. RESONANCE ABSORPTIONS

The resonance absorption of highly reflecting coated silver mirrors at certain IR frequencies has been studied in detail. The technique has been exploited as a new procedure for evaluating coating optical thickness and/or refractive index.

4. FUNDAMENTAL COATING ABSORPTION BANDS

The fundamental absorption bands of the coatings have been studied with special emphasis on the longitudinal band on the short wavelength side of the fundamental. Most of the work has been described in detail in References 3, 4, 5 and Appendix A. Some additional work included in this

---

1. W.N. Hansen, "Reflection Spectroscopy of Optical Coatings," J. Opt. Soc. Am., 69, 264 (1979).

2. W.N. Hansen, "Electric Fields Produced by the Propagation of Plane Coherent Electromagnetic Radiation in Stratified Medium," J. Opt. Soc. Am., 58, 380 (1968).

report is as follows. A general method for determining the optical constants of liquids is being developed. Progress has been made in implementing the use of causal transformations. Such data manipulation requires that spectra be digitized for computers. That capability is now available with requisite software working. The constants of liquid water have been determined to demonstrate proper use of system equipment and software and are compared herein with literature values. The ability to determine the optical constants of liquids is essential because constants of contaminating liquid materials (e.g., pump oil) are not generally available in the literature. Another important problem that needs theoretical and experimental investigation is the determination of how the spectral properties of contaminating molecules depend upon the matrix in which they are embedded. The beginnings of this problem are addressed in this report.

Please note that the scientific background to this research is discussed in AFWL-TR-79-197 of which this is a supplement.

---

3. W.N. Hansen, "Characterization of Small Absorptions in Optical Coatings," AFWL-TR-79-197, AirForce Weapons Laboratory, Kirtland Air Force Base, NM, (July 1980).

4. W.N. Hansen, Lee Pearson, Galen Hansen, and W.S. Anderson, "Characterization of Small Absorptions in Optical Coatings," NBS Special Publication 568, Laser Induced Damage in Optical Materials, H.E. Bennett, A.J. Glass, A.H. Guenther, and B.E. Newnam, editors, U.S. Government Printing Office, Washington, D.C., (1973).

5. W.J. Anderson and W.N. Hansen, "Reflection Spectroscopy Analysis of Surfaces and Thin Films," SPIE Proceedings, Vol. 276, D.E. Aspnes, S.So, and R.F. Potter eds., (1981) p. 214.

II. RESULTS

1. THE THORIUM FLUORIDE STORY: ADDITIONAL RESULTS

Additional studies of thorium fluoride (ThF_4) films were continued. The dominating physical feature remains the large amount of moisture present in the films. It had been supposed that the films were hygroscopic and had taken up water since preparation. Implications were that the ThF_4 films were very sensitive to ambient atmosphere humidity and that they would degrade rapidly. Further detailed measurements indicate, however, that this may not be the case. First, detailed calculation shows that the degree of water contamination is greatest at the inner interface rather than at the ThF_4-air interface. An example is discussed in detail later in this report. The presence of water mainly near the inner interfaces indicates that it did not come from the ambient atmosphere after preparation. Second, the ThF_4 films were soaked in a 100 percent humidity atmosphere at room temperature for a month. Typical results are shown by Figures 1 through 4. There is little change with exposure to this humid atmosphere. Therefore, the moisture must have originated in the preparation. This point was further tested by studies on another ThF_4 film that was specially prepared to exclude moisture. The moisture content was indeed less by a factor of about 40, and did not increase significantly by exposure to ordinary air.

An internal reflection spectrum taken at an internal 45 degree angle of incidence, θ_i, is shown in Figure 5. The detailed analysis of this film is given in the last section of this report. It is easy to see that the moisture observed had to be close to the inner zinc selenide (ZnSe)-ThF_4 interface because the sensing evanescent wave penetrates only about one-tenth of a wavelength into the ThF_4 which has an optical thickness of 4 μm.

2. CHARACTERIZATION OF IMPURITIES

Considerable progress has been made in the ability to identify, locate, and quantify small amounts of impurities in optical coatings. Typically, the impurities retain their characteristic fundamental oscillator strength signatures as a function of wavelength. It can then be assumed that the intrinsic spectra of the impurity species are the same as in their pure condensed matter state, whether they occur in the optical component as a separate film at an interface or dispersed throughout an optical layer. Preliminary spectral measurements help decide on an appropriate model of the system. Computer calculations on the digitized spectra then reveal the intrinsic impurity spectra, amounts, and location (Refs. 1, 3 to 5, 6 and 7). One case will be discussed at this point to illustrate the deconvolution of reflection spectra, to give true intrinsic

---

6. W.N. Hansen and W.A. Abdou, "Causality Calculations in Reflection Spectroscopy," J. Opt. Soc. Am., 67, 1537 (1977).

7. W.N. Hansen and W.A. Abdou, "Analysis of Solid Liquid Interphase Spectra via Causal Transformation," J. Phys. (Paris), 38, C5-207 (1977).

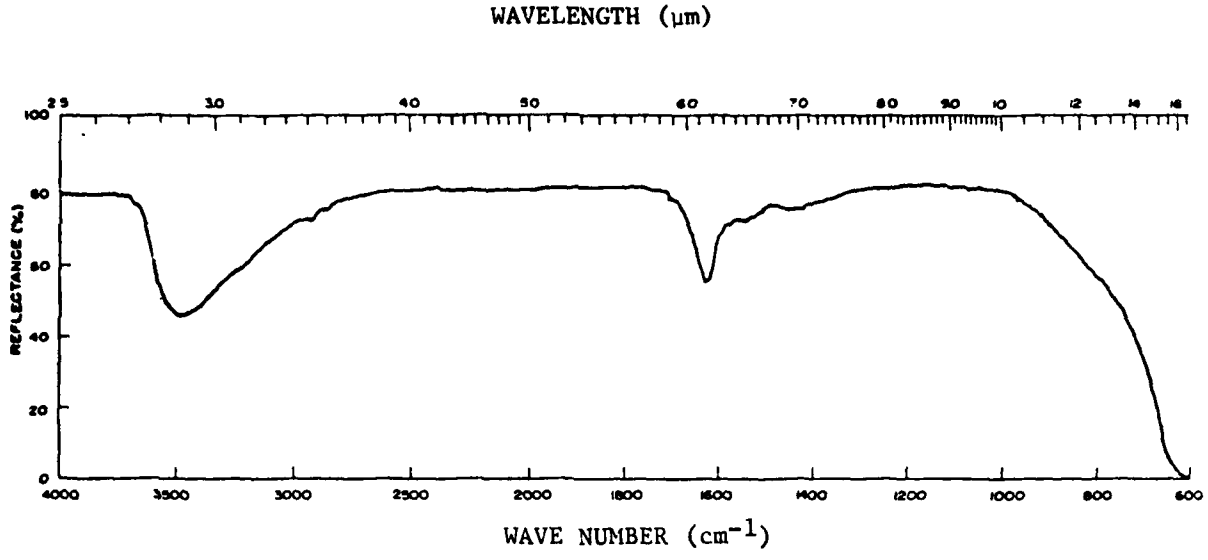

Figure 1. Multiple internal reflection spectrum of sample 8071-B taken at a 45-deg internal angle of incidence. ZnSe plate with 4000 Å ThF_4 film, 25 reflections.

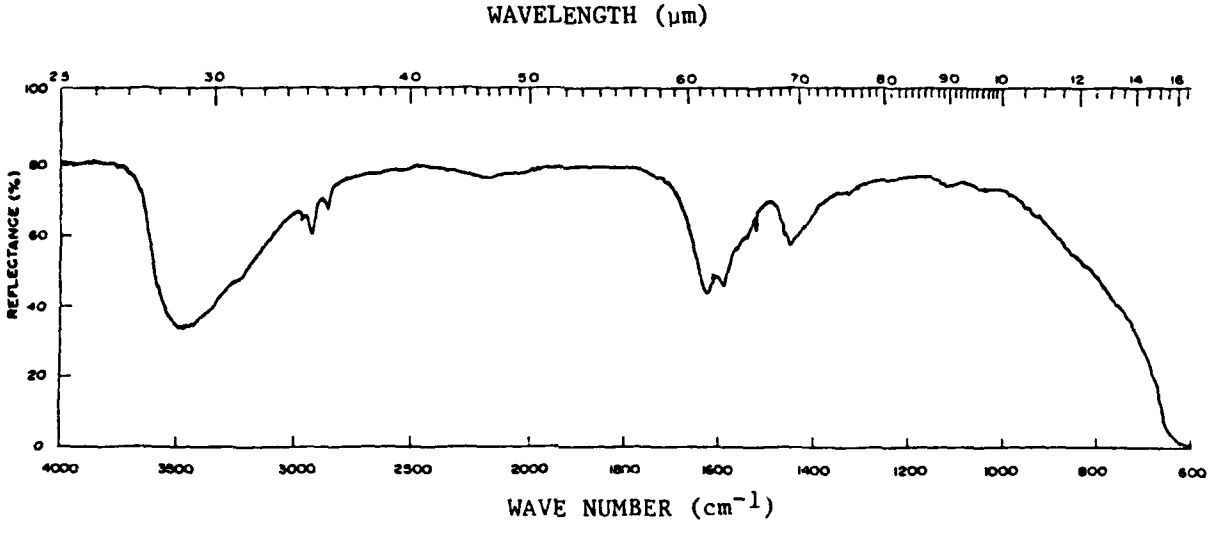

Figure 2. Multiple internal reflection spectrum of sample 8072-B taken at a 45-deg angle of incidence. ZnSe plate with 3000 Å ThF_4 film capped with 1000 Å of CeF_3, 25 reflections.

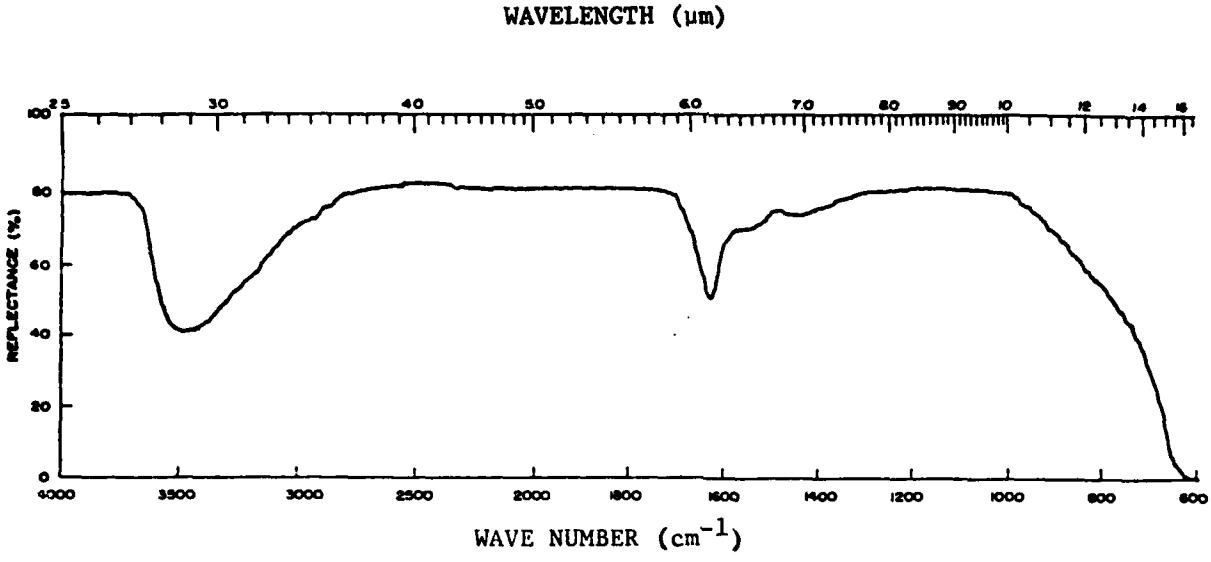

Figure 3. Same as Figure 1 but after sample was soaked 1 mo in air at room temperature and 100 percent relative humidity.

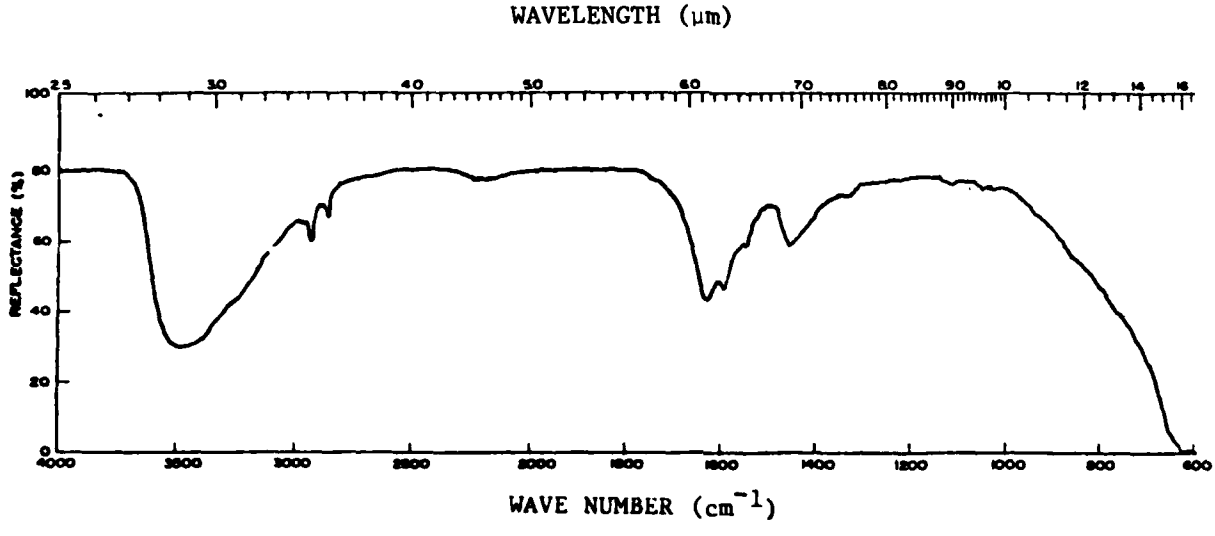

Figure 4. Same as Figure 2 but after sample was soaked 1 mo in air at room temperature and 100 percent relative humidity.

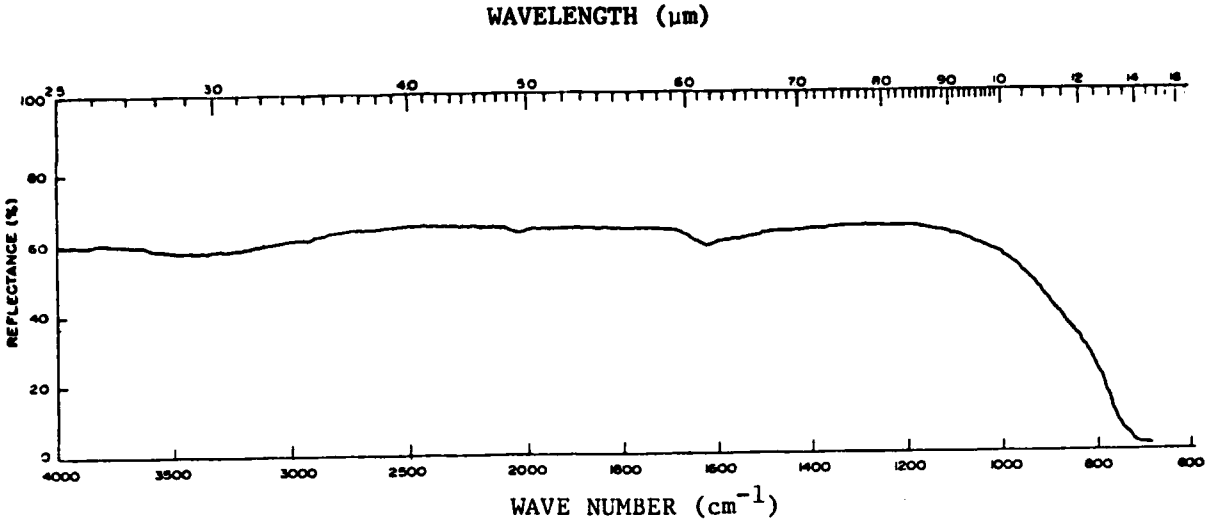

Figure 5. Multiple internal reflection spectrum of 2.56 micron ThF_4 film on ZnSe plate; 45 deg; 25 reflections.

spectra of small amounts of impurity. The deconvolution is possible even if the spectra differ from the traditional transmission spectral signature. The raw spectra are shown in Figure 6. The sample is spiked with 100 Å of silicon monoxide (SiO). Using a causal transformation and established procedures, the intrinsic spectra (Fig. 7) are obtained and compared with spectra obtained from literature (dashed lines) for SiO. There is a frequency shift, probably due to the unusual environment in which the SiO finds itself, but the signature is clear. There is also a hint of an SiO_2 band. This is not surprising as SiO tends to absorb oxygen when evaporated.

Another important technique, that of quantitatively determining the amount of one impurity in the presence of others, is illustrated in Figure 8. The characteristic oil spectrum (between 2800- and 3000- cm^{-1}) almost always seen in sensitive spectra of optical coatings, overlaps the large water band. Also, the 100 percent line is not constant but varies slowly compared to the oil spectrum. Neither of these interferring spectra prevent quantitative determination of the oil amount. A line is simply drawn to reproduce what the spectrum would be without the oil bands. The new spectrum serves as the bleached spectrum in the casual transformation procedure. If the oscillator strengths or polarizabilities of the oil molecules are known, their concentration can be calculated. These quantities can be calculated from the determined optical constants of the liquid oil.

3. DETERMINING THE OPTICAL CONSTANTS OF LIQUID: WATER AT ROOM TEMPERATURE

The optical constants of a liquid can be calculated from a transmission spectrum taken through a liquid filled variable path-length cell. The method is as follows. A spectrum of the sample is taken at a particular path-length setting of the cell; a second spectrum is taken at another path-length setting. The log of the ratio of the two spectra gives the absorbance of a sample whose thickness equals the difference in path-length of the two settings. The window material is chosen so that its index of refraction is close to that of the liquid, thus reducing any interference pattern caused by reflection from the two liquid-window interfaces. Also, if the liquid is absorbing in the spectral region being scanned, light will be attenuated and thus further reduce any interference pattern to an almost nonexistent state. Hence, it is not essential to use the index of refraction of the windows in calculating the complex index of refraction ($\hat{n} = n+ik$) for the liquid.

The transmittance for the liquid is given by

$$T = I/I_o \equiv \exp(-ah) \tag{1}$$

where

$$a = 4\pi k/\lambda \tag{2}$$

and is referred to as the absorption coefficient. h is the difference in path-lengths of the two settings and λ is the wavelength of the incident light in vacuum. Transmittance absorbance is defined as

$$A = -\log_{10}(T) = -\ln(T)/\ln(10) = 4\pi kh/\lambda\ln(10) \tag{3}$$

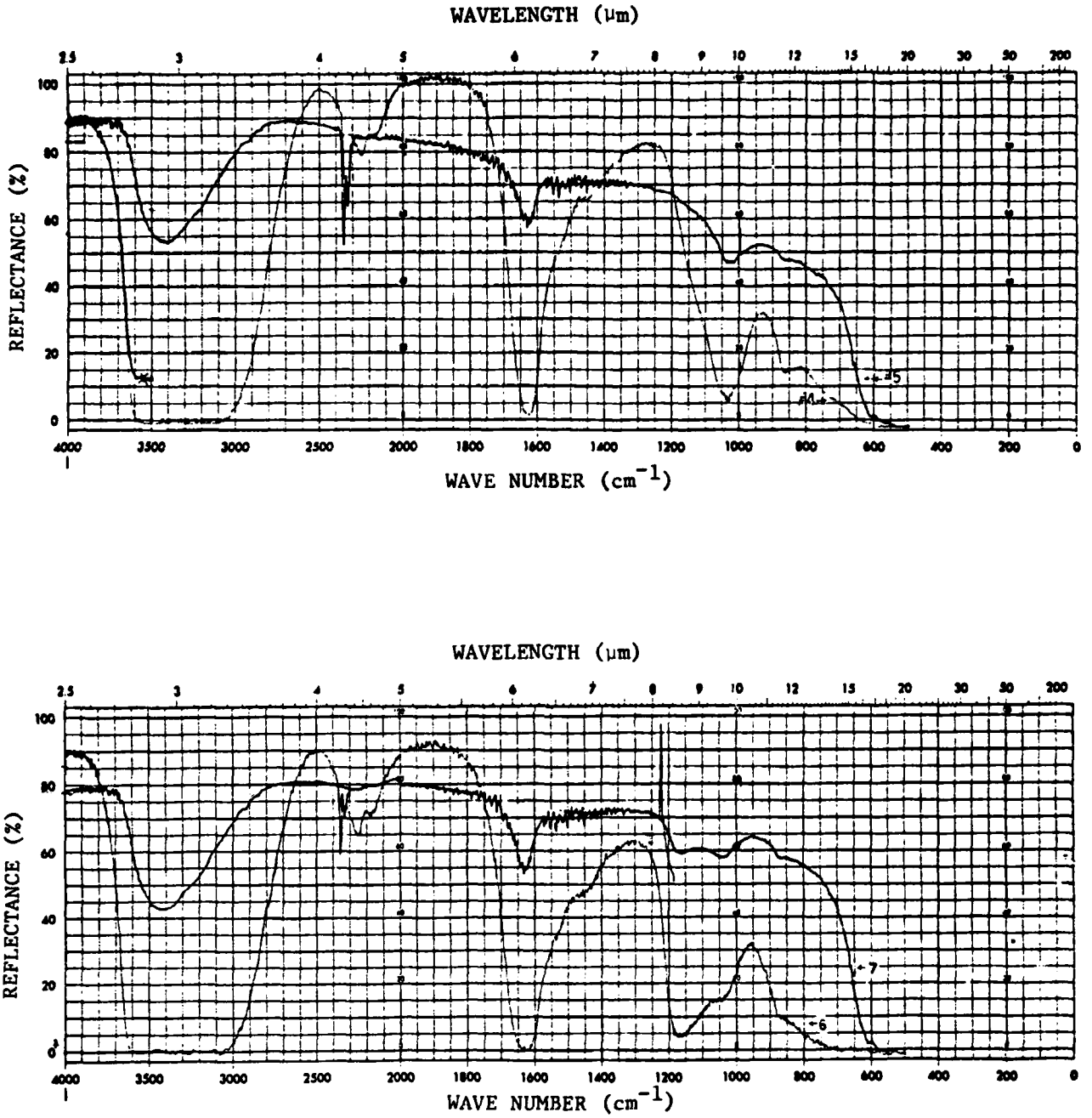

Figure 6. Internal reflection spectra of ThF_4 on ZnSe plate with 100 Å of SiO under the ThF_4. Curve 4 is $\perp$ polarization, θ_i = 30 deg, 20.3 reflections. Curve 5 is $\perp$ polarization, θ_i = 71.8 deg, 3.7 reflections. Curve 6 is || polarization, θ_i = 30 deg, 20.3 reflections. Curve 7 is || polarization, θ_i = 71.8 deg, 3.7 reflections.

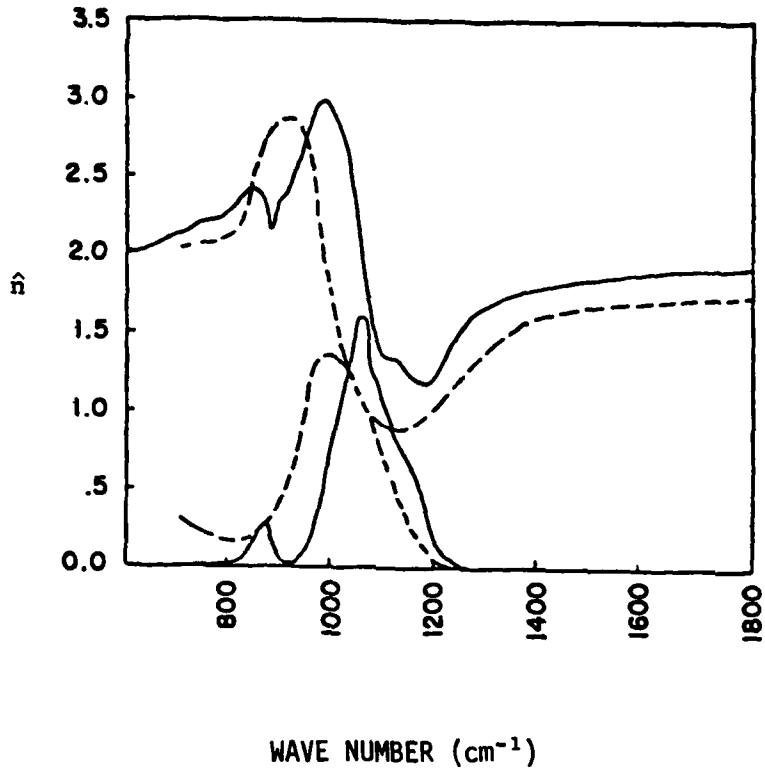

Figure 7. Complex index of refraction of the 100 Å SiO layer as determined from the data of Figure 6. The upper solid curve is n and the bottom solid curve is k. The dashed curve is for pure SiO and was obtained from literature.

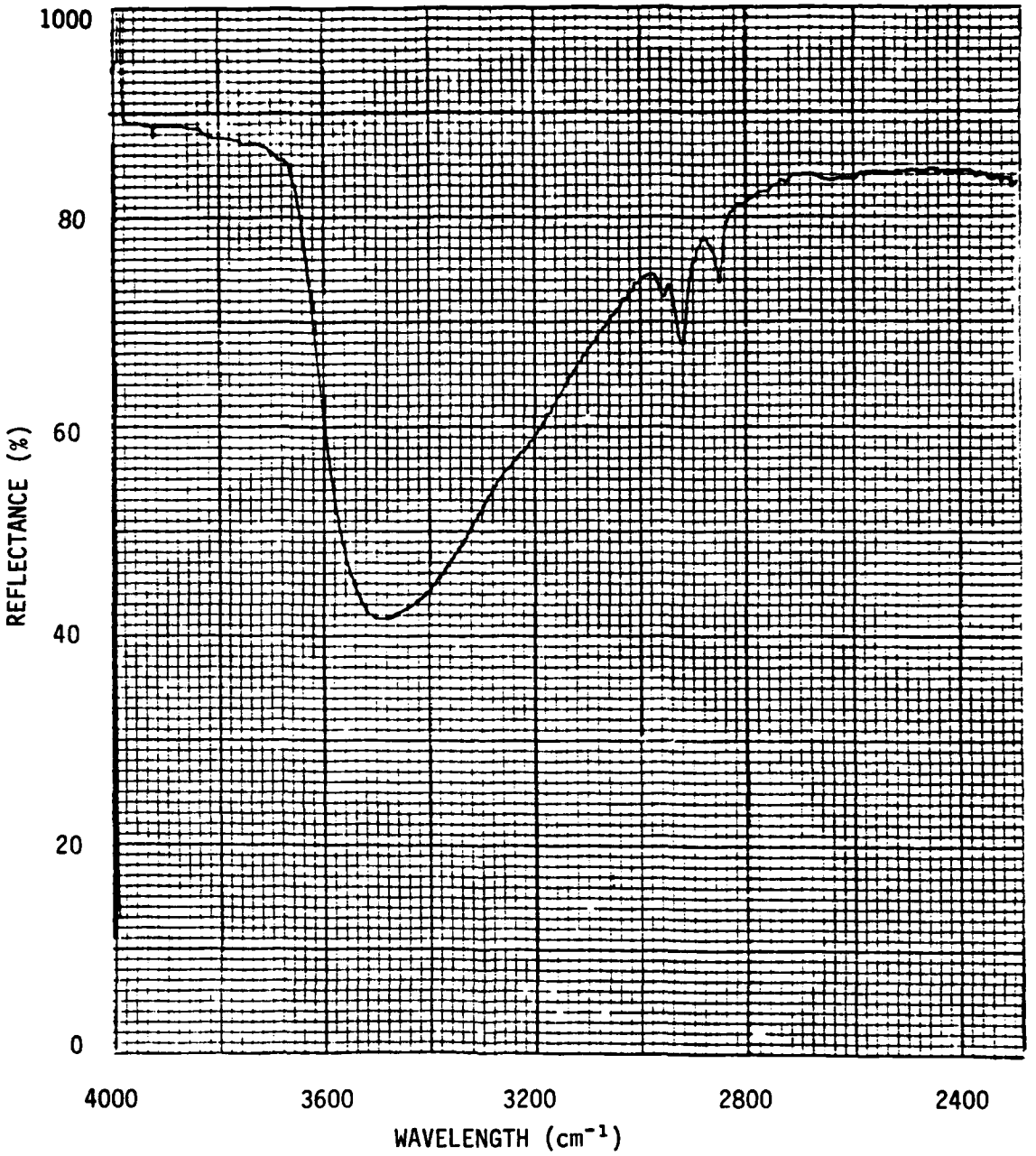

Figure 8. Internal reflection spectrum of 3000 Å ThF_4 on 45 deg ZnSe plate. ThF_4 film is covered by 1000 Å of CeF_3. θ_i = 45 deg is greater than θ (critical) = 38.3 deg, for the ZnSe-ThF_4 interface. Large H_2O band seen with superimposed pump oil band in the 2800-3000 cm^{-1} region.

Solving for k gives

$$k = A\lambda \ln(10)/4\pi h \tag{4}$$

It is possible to calculate n directly from the k calculated by Equation 4. This calculation is made by either a Krammers-Kronig analysis or by using the Peterson-Knight (PK) (Ref. 8) transformation. If the PK method is used then a causal function must be defined. The function $\hat{n} - 1 = (n-1) + ik$ is causal, i.e., its real and imaginary parts are related by the PK transformation. Hence, transforming k yields n-1. Adding 1 to this result gives n for the liquid, and now n and k are known over a certain wavelength range (Refs. 6 and 7).

Actually, since transmittance and/or reflectance spectral data always extend over only a finite wavelength range, auxilliary data are required to calculate n from the spectrum-derived k. This requires special techniques discussed in References 6 and 7. This procedure is now discussed briefly. The concept of an electromagnetically bleached sample, denoted by subscript b, is invoked.

It is convenient to write

$$k-k_b = (A-A_b)\lambda \ln(10)/4\pi h \tag{5}$$

But k_b is zero by definition, and

$$k = (A-A_b)\lambda \ln(10)/4\pi h \tag{6}$$

The bleached *sample is bleached* only in the range of the measurement. Outside that range it has the same k as the real sample. Since the difference between two causal functions is causal, $(\hat{n}-\hat{n}_b)$ is a causal function. Therefore, the real part can be determined by a causal transformation from the imaginary part. $\mathrm{Im}(\hat{n}-\hat{n}_b) = (k-k_b) = k$ is known at all wavelengths. Therefore, $\mathrm{Re}(\hat{n}-\hat{n}_b) = n - n_b$ can be calculated at all wavelengths. To determine $\hat{n}$ throughout the experimental wavelength range it is necessary only to determine n_b in that range, in addition to the above derived information, that is, in addition to k and $n-n_b$. But n_b is a simple function, essentially linear over the experimental range. It need only be determined at two points and then be linearly interpolated. This can be done by determining n of the real sample at two points, since $(n-n_b)$ is known. This auxilliary information must be obtained, however, since it is not contained in any single spectrum.

To illustrate these procedures, consider water. Figure 9 is a transmission spectrum of 2 μm of water. Figure 10 shows spectral values of n and k (line) calculated from experimental data. These values are compared with literature (Ref. 9) values (dots) obtained by other means.

---

8. C.W. Peterson and B.W. Knight, J. Opt. Soc. Am., 63, 238 (1973).

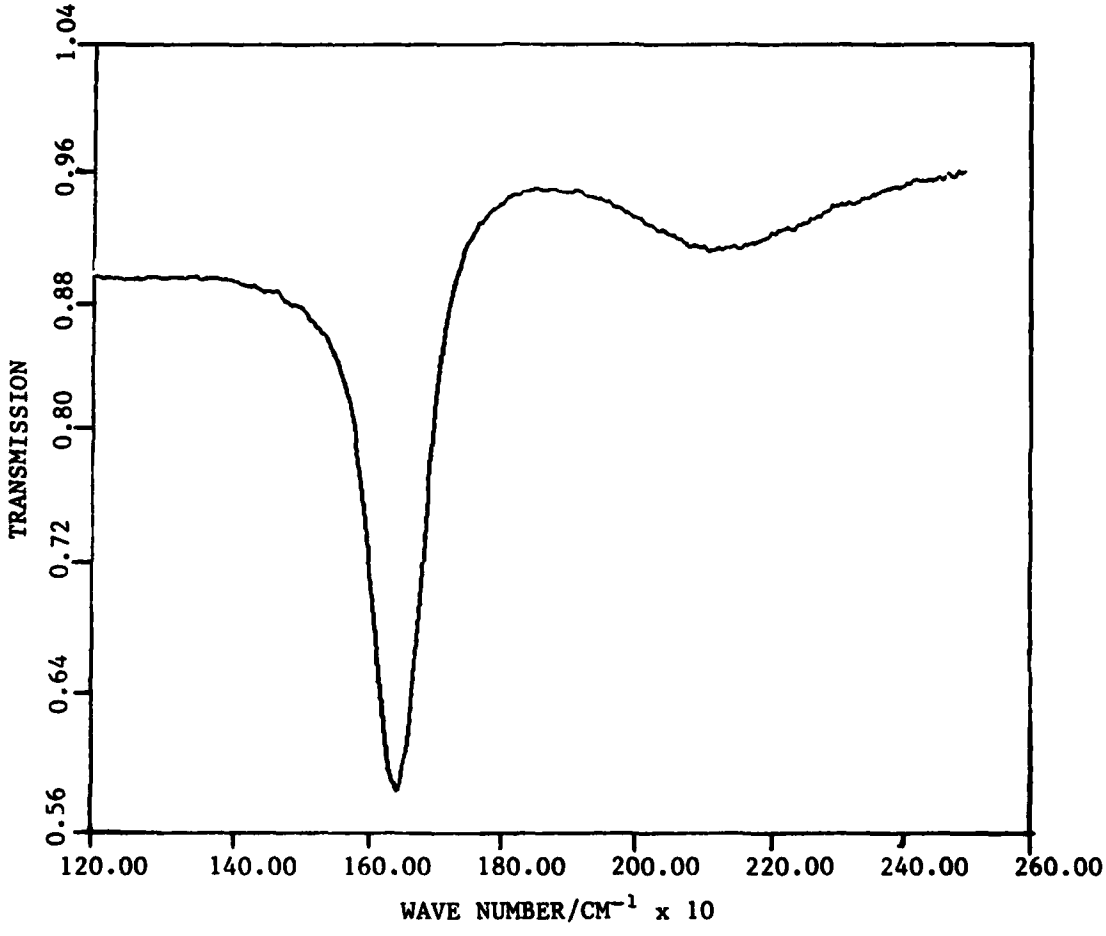

Figure 9. Transmission spectrum of pure liquid water about 2.0 μm thick. Data were determined and manipulated by a Nicolet FTIR instrument and plotted with a computer system. Two spectra for thicknesses differing by 2 μm were used.

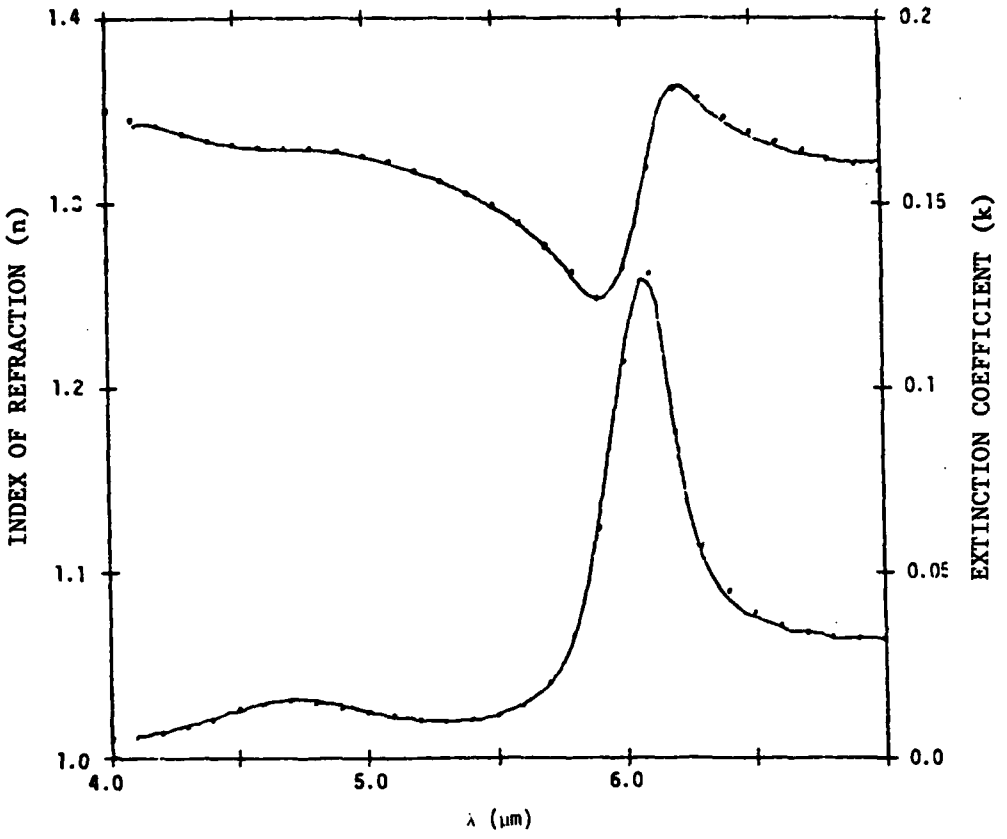

Figure 10. A comparison of n and k spectral values for water as determined from Nicolet FTIR measurements (lines) and literature values (points).

The objective here is not necessarily to improve the known optical constants of water, but to develop and prove a convenient versatile method. The resultant method is both convenient and versatile.

4. ANALYSIS OF SILICON NITRIDE ON Ge SAMPLE

A multiple internal reflection spectrum taken at a 30 degree angle of incidence is shown in Figure 11 for the silicon nitride (Si_3N_4) on germanium (Ge) sample. The first phase is Ge, the second is an 800 Å film of Si_3N_4 and the third is air. Note the water band with maximum at 3350 cm^{-1} and also the hydrocarbon bands at 2970, 2930, and 2850 cm^{-1}. These impurity bands are found, to greater or lesser degrees, in virtually all of the samples that have been examined. The large absorption band at 2180 cm^{-1}, or approximately 4.6μm, is not an intrinsic Ge or Si_3N_4 band but arises from the presence of SiH (silicon hydride) which is a by-product of the Si_3N_4 production process. According to G. Socrates (Ref. 10) the SiH stretching mode gives rise to a strong absorption band in the 4.44 to 4.76 μm region (the center of which is 4.6 μm). Figure 12 is a chart taken from Reference 11 and shows the region of the SiH band and indicates its relative strength.

5. IMPURITY CALCULATIONS USING POLARIZABILITY AND LORENTZ LOCAL FIELD THEORY

The concentration of an impurity molecule such as H_2O in a ThF_4 matrix can be estimated by rationing the extinction coefficient, k (measured for the impure sample) to the k of the pure matrix material. Actually this is easy to do if intrinsic absorption bands of the impurity and the matrix substance do not overlap. This calculation is intuitatively a good first approximation but may not be very accurate because the space-time average field $\langle E \rangle^2$ seen by the water molecule depends on the matrix in which it finds itself. A more accurate way to calculate impurity concentrations is to use the solid state theory of polarizability.

The polarization of a material is related to its polarizability by the equation

$$P = NaE_{loc} \tag{7}$$

where a is the polarizability, E_{loc} is the local electric field and is the field actually seen by a given molecule, and N is the concentration of molecules per unit volume. The local field is calculated using a model

---

9. G.M. Hale and M.R. Querry, "Optical Constants of Water in the 200-nm to 200- m Wavelength Region," App. Opt., 12, 555 (1973).

10. G. Socrates, "Infrared Characteristic Group Frequencies," p. 126.

11. Handbook of Chemistry and Physics, 53rd edition, 1972-1973, p. F-200.

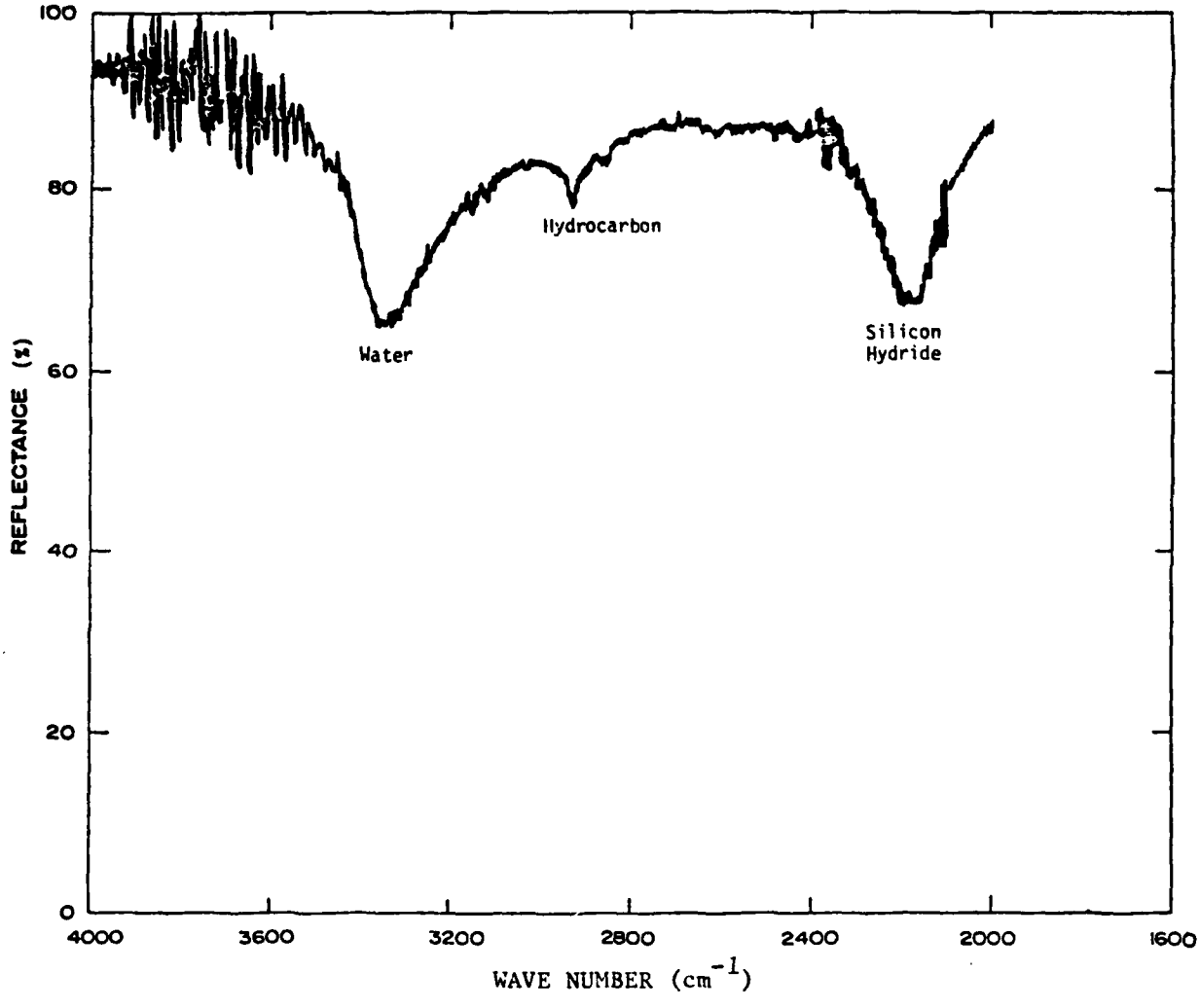

Figure 11. Multiple internal reflection spectrum of 800 Å Si_3N_4 film on 30 deg Ge plate with 43 reflections.

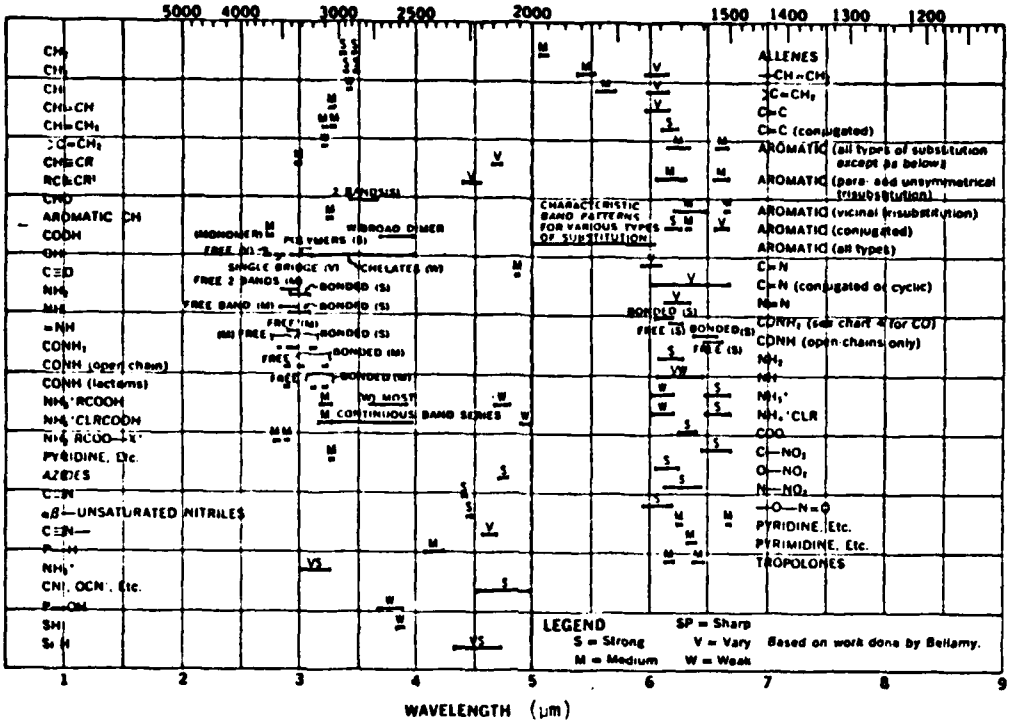

Figure 12. Infrared correlation chart. This chart presents some information regarding structure, double-bond vibrations, hydrogen stretching and triple-bond vibrations (Ref. 11).

$$E_{loc} = E + 4\pi P/3 \tag{8}$$

where E is the electric field inside the material and is calculated using the boundary conditions derived from Maxwell's equations for electric fields. Substituting Equation 8 into Equation 7 and solving for P gives

$$P = NaE/(1-4\pi Na/3) \tag{9}$$

Recall that the electric displacement vector is related to the electric field and the polarization by the equation

$$D = E + 4\pi P \tag{10}$$

For isotropic materials and for the magnetic permeability being unity

$$D = \hat{n}^2 E \tag{11}$$

where $\hat{n}$ is the complex index of refraction. The following result is obtained by combining Equations 9, 10, and 11.

$$(4\pi/3)Na = (\hat{n}^2 - 1)/(\hat{n}^2 + 2) \tag{12}$$

Equation 12 is commonly referred to as the Lorentz-Lorenz equation and relates the microscopic quantity, a, to the macroscopic quantity, $\hat{n}$. If there are impurities present and if the assumption is made that all species of molecules see the same local field due to a sufficiently short range homogeneity of the material, then Equation 12 can be written in the form:

$$(4\pi/3)\sum_i N_i a_i = (\hat{n}^2 - 1)/(\hat{n}^2 + 2) \tag{13}$$

In Equation 13, $\hat{n}$ is the complex index of refraction for the composite material. The polarizabilities, a_i, for each species can be calculated from the measured $\hat{n}$ using Equation 12. It should be noted here that it is assumed that the polarizability is a molecular parameter and is unchanged by the molecule's environment. With the measured complex $\hat{n}$ for the composite material, Equation 13 can be used to estimate the impurity concentrations.

The type of samples considered here are multiple internal reflection plates which are typically made of the substrate ZnSe with identical films coated on each side. The films of interest are made of ThF_4. The most common impurities found in ThF_4 are water and hydrocarbons such as pump oils.

For films which are not homogeneous and whose impurity concentrations are not higher than a few percent at any location the real part of the index of refraction n, is essentially constant throughout the film and is equal to the n of the pure material. On the other hand the imaginary part of the index of refraction, k, is a strong function of impurity concentration near absorption bands of impurities and when calculated from

---

12. Ali Omar, "Elementary Solid State Physics," pp. 376-384.

reflection spectra, varies with the angle of incidence of the incident light for films in which the impurity is not uniformly distributed. Because the electric field configuration in the film is dependent on the angle of incidence it is essentially looking at different regions of the sample as the angle of incidence varies. The dependence of k on the angle of incidence can, therefore, be interpreted as a spacial dependence. If the film is homogeneous in directions parallel to its planar interface with other layers then k takes on only a z dependence where z is the direction through the film perpendicular to its interfaces, i.e., k becomes k(z). To approximate k(z) the approximate values of z corresponding to the measured k values are determined by calculating a center of gravity of the $\langle E^2 \rangle$ fields, that is, z is determined using the equation

$$z = \sum_i \langle E^2 \rangle_i z_i / \sum_i \langle E^2 \rangle_i \qquad (14)$$

Once k(z) and n(z) are known, it is possible to calculate the concentration, N(z) for the impurity molecule using Equation 13. N(z) is assumed to be constant for the matrix molecule and equal to its intrinsic value.

Figure 13 shows (for a ZnSe substrate sample with a 3.84 μm optical thickness film of ThF_4) the percentage of molecular water contamination as a function of z. The z dependence was approximated by Equation 14. Several reflection spectra at various settings were used in these calculations. Figure 5 shows the multiple internal reflection spectrum of this sample with a 45 degree angle of incidence. Figure 14 is a transmission spectrum showing the interference pattern due to the ThF_4 film. This spectrum was used to calculate the film thickness by a method discussed in Appendix A.

Figure 13 shows two curves representing measurements taken at the 1640 (upper) and 3400 (lower) wave number absorption bands of water. The disparity in the two curves is likely due to the water molecules bonding to the ThF_4 molecules in such a way that either the 3400 wave number oscillation is inhibited or that the 1640 wave number oscillation is enhanced. Since there is no proven theory for these oscillator strength changes, the simplest way to approximate the percentage of water molecules is to average the two curves, hence the following was done. The curves were each fit to an exponential function by a least-squares method, then averaged and the resultant exponential function was integrated over the thickness of the film to obtain the total percentage of water molecules. This process gives a value of 0.14 percent water molecules, by number. The water concentration is greatest at the ZnSe-ThF_4 interface (z=0) and decreases away from the interface. The same procedure was used to calculate the total percentage of water in the 8071-B (ZnSe-ThF_4) and 8072-B (ZnSe-ThF_4-CeF_3) samples. Figures 1 and 2 are multiple internal reflection spectra of these two samples taken at a 45 degree incidence angle. In these cases the curves that best fit the data were linear (Fig. 15). The total percentage of water molecules in sample 8072-B is approximately 7 percent and that of sample 8071-B is approximately 8 percent. In both samples z=0 represents the ZnSe-ThF_4 interface. The ThF_4 film of sample 8071-B is actually 0.4 μm thick; however, only the first 0.3

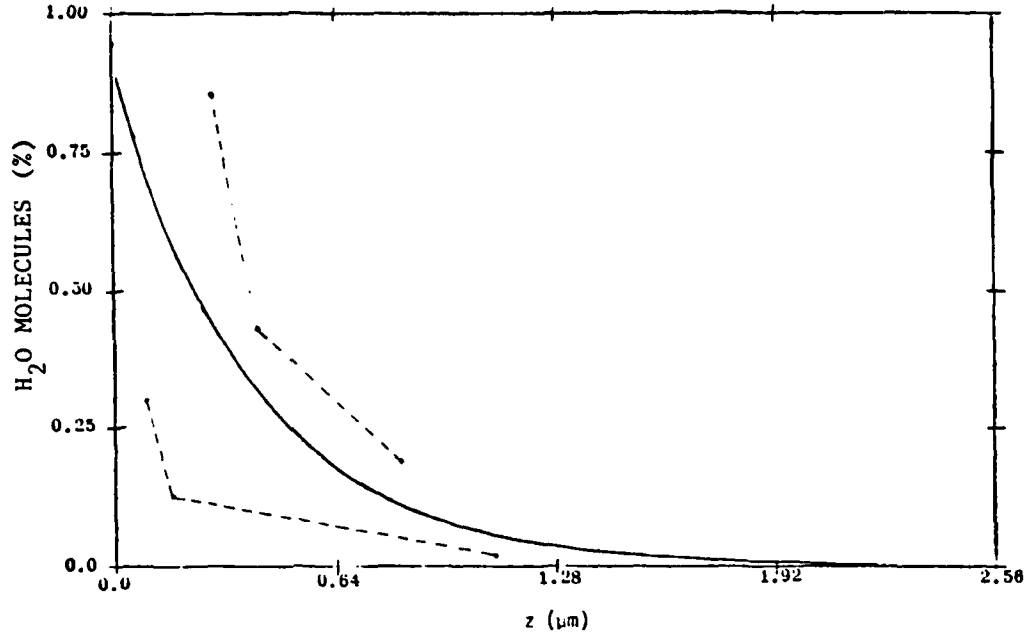

Figure 13. Percentage of water molecule contamination (by molecular count) as a function of position in the ThF_4 film of Figure 5. The upper curve uses the 1640 cm^{-1} water band data and the lower curve uses the 3400 cm^{-1} water band data. The solid curve is the average of the exponential fits to the two dashed curves.

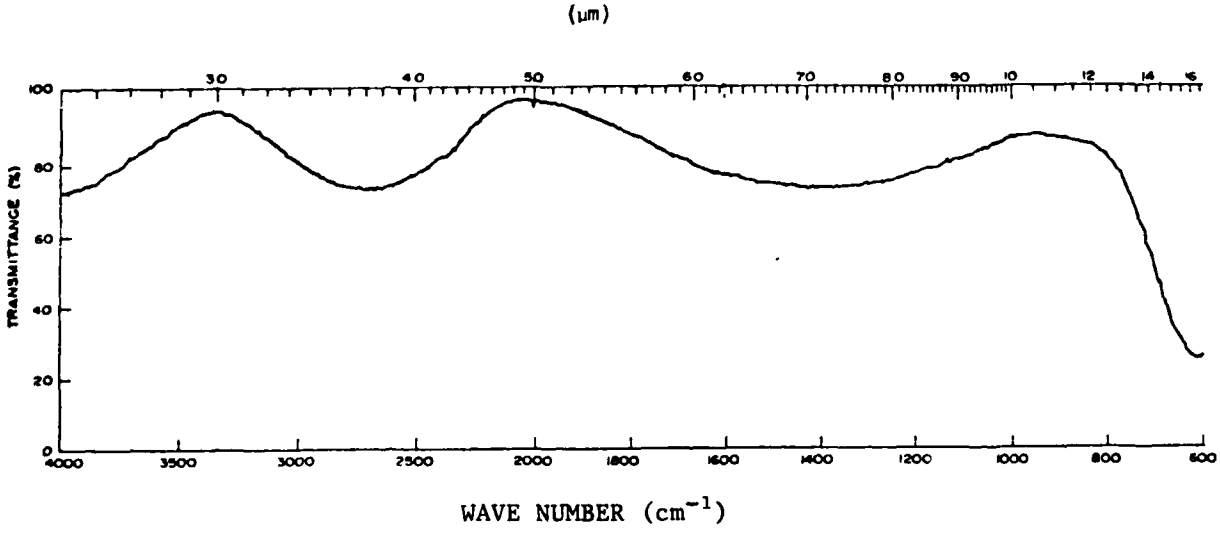

Figure 14. Transmission spectrum of the Figure 5 sample showing the interference pattern resulting from the ThF_4 film.

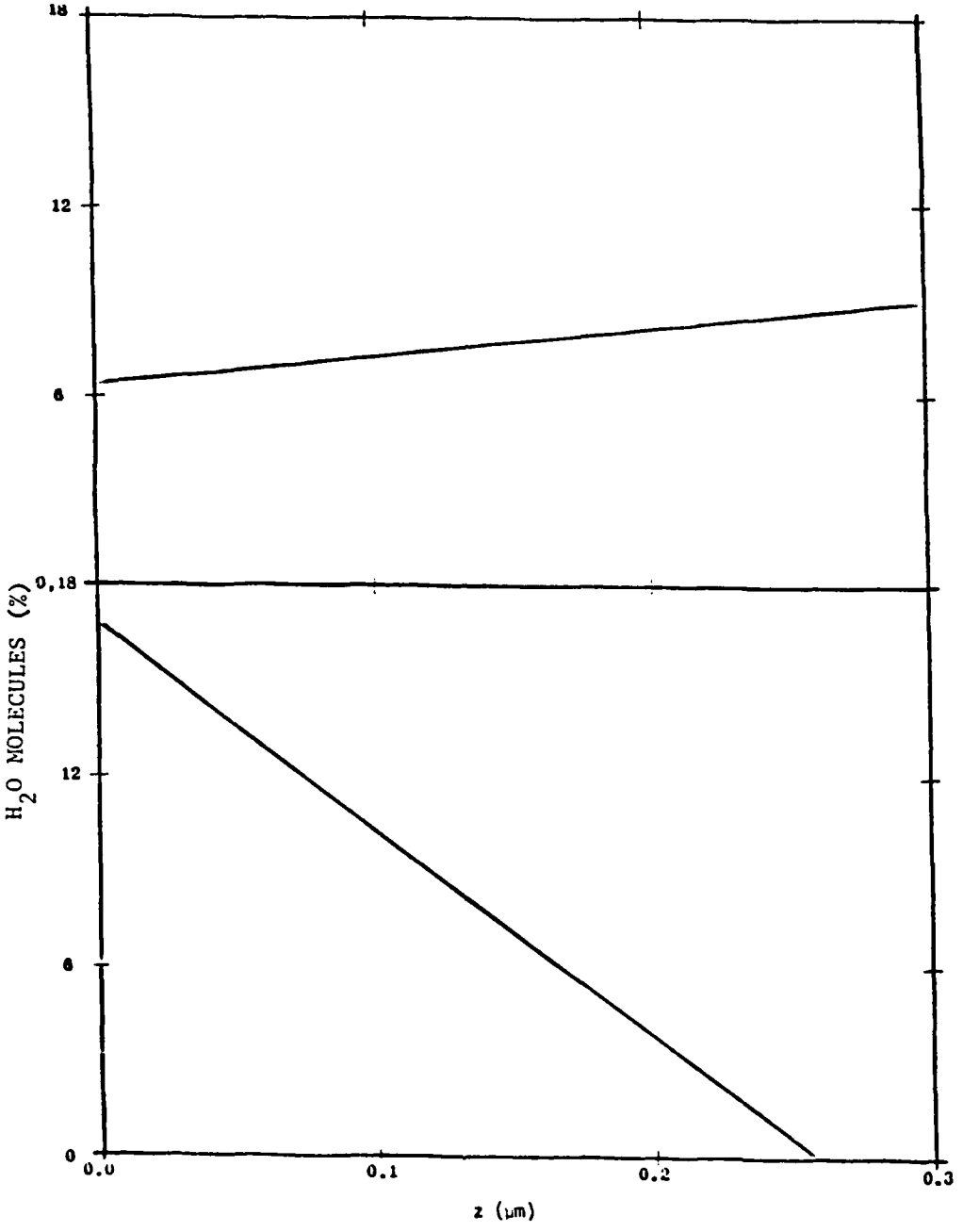

Figure 15. Water molecule impurity concentration versus position in the ThF_4 films of Figures 3 (upper curve) and 4 (lower curve), as determined by the center of gravity method.

μm are plotted. The water concentration in this film is increasing away from the ZnSe-ThF_4 interface. In sample 8072-B the water concentration is decreasing away from a=0 in the ThF_4 film. Both of these samples were placed in a 100 percent humidity atmosphere for 1 month prior to the time the preceeding measurements and calculations were made. Figures 3 and 4 are multiple internal reflection spectra taken of samples 8071-B and 8072-B after the 1 month soaking period. Therefore, it appears that the 0.1 μm cap of CeF_3 on the ThF_4 film of sample 8072-B inhibited the diffusion of water into the ThF_4. A quanitative comparison of Figures 1 and 2 with Figures 3 and 4 reveals a change in absorptance of 22.9 percent at the 3400 cm^{-1} band and 20.8 percent at the 1640 cm^{-1} band for sample 8071-B. For sample 8072-B the change in absorptance is 14.3 percent and 6.2 percent for the 3400 cm^{-1} and 1640 cm^{-1} bands. This further indicates that the CeF_3 cap reduced the diffusion of water into the ThF_4 film of sample 8072-B.

Absorptance is defined as

$$A = 1-R \tag{15}$$

where R is the reflectance. Since the absorptance at the two water bands cited above is almost entirely due to the water impurity in the ThF films of the two samples, the following equation can be used to represent the absorptance (Ref. 1).

$$A = \frac{4\pi h}{\lambda} \frac{nk}{n_1 \cos\theta_1} \langle E^2 \rangle_f \tag{16}$$

$\langle E^2 \rangle_f$ is the space-time average electric field in the film and n, k and h are respectively, the index of refraction, extinction coefficient, and thickness of the film. The quantities n_1 and θ_1 are respectively, the index of refraction of the first phase and the angle of incidence upon the interface between the first and second phases. It is evident from Equation 16 that the absorptance, A, is proportional to k, the extinction coefficient. k, on the other hand, is approximately proportional to the impurity concentration and, therefore, A is approximately proportional to the impurity concentration.

From this information, the conclusion is drawn that the moisture content of sample 8071-B exhibits an increase on the order of 20 percent and that of 8072-B increased on the order of 10 percent during the 1 month, 100 percent humidity soak.

III. CONCLUSIONS AND RECOMMENDATIONS

The results obtained indicate that thorium flouride films are not necessarily hygroscopic and may be quite stable in ordinary air. They are prone to contain important amounts of moisture which absorbs strongly at important laser wavelengths. The presence of water is undoubtedly due to preparation procedures. Thorium halides react readily with water at high temperatures to form thorium oxide and/or oxyhalides. Any water in the evaporation feed stock would probably contaminate the films and could also cause thorium oxide and/or oxyflouride to be present in the optical films.

While this research did not directly address this point, it is known from inorganic chemistry that pure anhydrous ThF_4 can be prepared and kept that way during film preparation. The resulting optical films will not contain water, and will probably not absorb moisture if they are prepared completely dry. Spectroscopic techniques like those employed in this work are a very sensitive test of dryness and the ability to remain that way. The feedstock itself could be examined spectroscopically for moisture and structural information.

It is now fairly routine to identify absorbing impurity species and determine their approximate amounts and positions, even in the presence of other absorbing species. Improvements are still needed in all these determinations, but especially in pinpointing the impurity location nondestructively. Further knowledge of the effects of the matrix on oscillator strength will help increase the accuracy in determining the amount of impurities present. Temperature effects need to be examined in detail.

Procedural advances, including bit-pad digitization of graphical spectra are helping to make the optical characterization of liquids in the infrared more of a routine matter. Similarly, causal transformation procedures are used with liquids and multilayer optical coatings. These procedures are useful in characterizing condensed phase material that might cause contamination in optical fabrication.

For the present work there is usually plenty of spectral resolution. An important limitation in these procedures is the infrared spectrophotometer. However, in this work, spectrophotometers are always being pushed to the limit in terms of sensitivity and photometric accuracy. Usually they are also limited in sample type capability, having been designed for routine transmission work. Data handling capability is very important. Spectra routinely need to be simultaneously co-added, subtracted, ratioed and especially Fourier transformed.

REFERENCES

1. W. N. Hansen, "Reflection Spectroscopy of Optical Coatings", J. Opt. Soc. Am. , 69, 264 (1979).

2. W. N. Hansen, "Electric Fields Produced by the Propagation of Plane Coherent Electromagnetic Radiation in Stratified Medium", J. Opt. Soc. Am. , 58, 380 (1968)

3. W. N. Hansen, "Characterization of Small Absorptions in Optical Coatings," AFWL-TR-79-197, Air Force Weapons Laboratory, Kirtland Air Force Base, NM, (July 1980).

4. W. N. Hansen, Lee Pearson, Galen Hansen, and W. S. Anderson, "Characterization of Small Absorptions in Optical Coatings," NBS Special Publication 568, Laser Induced Damage in Optical Materials, H. E. Bennett, A. J. Glass, A. H. Guenther, and B. E. Newnam, editors, U. S. Government Printing Office, Washington, D. C. (1973).

5. W. J. Anderson and W. N. Hansen, Reflection Spectroscopy Analysis of Surfaces and Thin Films, in Proceedings of SPIE, Vol. 276m D. E. Aspnes, S. So, and R. F. Potter eds., (1981) p. 214.

6. W. N. Hansen and W. A. Abdou, "Causality Calculations in Reflection Spectroscopy, "J. Opt. Soc. Am. , 67, 1537 (1977).

7. W. N. Hansen and W. A. Abdou, "Analysis of Solid Liquid Interphase Spectra via Causal Transformation," J. Phys. (Paris), 38, C5-207 (1977).

8. C. W. Peterson and B. W. Knight, J. Opt. Soc. Am. 63, 238 (1973).

9. G. M. Hale and M. R. Querry, "Optical Constants of Water in 200-nm to 200-μm Wavelength Region," App. Opt., 12, 555 (1973).

10. G. Socrates, "Infrared Characteristic Group Frequencies," p. 126.

11. Handbook of Chemistry and Physics, 53rd edition, 1972-1973, p. F-200.

12. Ali Omar, "Elementary Solid State Physics," p. 376-384.

APPENDIX A

ABSORPTION DUE TO INTERFERENCE AND IMPURITIES IN THIN FILMS OF HIGH-ENERGY LASER OPTICS

SUMMARY

By using IR spectroscopy with external reflection techniques, significant causes of absorption were found in thin films on mirrors. The films studied are those used for enhanced and antireflection coatings on mirrors, windows and lenses of high-power lasers. Unexpectedly large amounts of water were found inside ThF_4 films. More importantly, a cause of absorption was found which has nothing to do with the quality of the film, but is due to interference in the film. The observed absorbances are large enough to cause significant damage to optical components in high-power lasers.

An equation is derived which describes the reflectance of the interference absorption band, and locates the max and min reflectance for a given film at some angle-of-incidence. Computer and spectral analysis show that varying the conditions of the sample and light will eliminate the absorption due to interference. However, enhancement of the minimum reflectance due to interference is shown to be a useful analytical tool in studying thin film absorbances.

I. INTRODUCTION

1. LASER DAMAGE DUE TO ABSORPTION

A major problem in the development of high-energy lasers is damage to optical components due to the absorption of light. The high intensity of the laser light causes otherwise insignificant absorptions to be fatal flaws in mirrors, lenses, and windows. Extensive research covering all types of absorbing species in optical components (e.g., surface roughness, inherent optical characteristics such as a nonzero extinction coefficient, substrate impurities, crystaline defects, etc.) is in progress worldwide (Ref.A-1). Absorption in the thin films used with optical componentsis especially important. It is this class of absorption with which this appendix is concerned. Absorptances as low as 10^{-4} can be significant (Ref. A-2).

The research discussed here was done during the summer of 1979 at the Naval Weapons Center (NWC) at China Lake, California. This appendix deals mainly with the discovery of absorption due to interference in thin films on mirrors. Also discussed are H_2O and hydrocarbon impurities found in some films. External reflection techniques were used to analyze the films and learn the location and contribution of absorbing species. Such films are used on mirrors as enhanced-reflection coatings, with several layers of films on top of each other. They are also used as antireflection coatings on windows and lenses, and for protection.

Decreases in the reflectance of films are commonly due to impurities such as H_2O and hydrocarbons (Refs. A-2 and A-3) and inherent vibrational bands of the film material such as those of ThF_4 at 350 cm^{-1}, and of zinc sulfide (ZnS) at 350 cm^{-1} and 265 cm^{-1}. However, the discovery of large absorption bands due to interference was totally unexpected, and for a little while unexplained. But it was found that not only can this absorption be eliminated, but enhancement of the interference band can be a useful tool in studying thin films.

2. EXTERNAL REFLECTION THEORY

To study thin films on mirrors and to analyze the resulting absorbances, a technique is needed which is sensitive, and produces good data which are both qualitative and quantitative, and are easily reducible.

A-1. "Laser Induced Damage in Optical Materials," Eds. A.I. Glass and A.H. Guenther, National Bureau of Standards (U.S.) Special Publication Nos. 414 (1974), 435 (1975), 462 (1976), 509 (1977).

A-2. W.N. Hansen, J. Opt. Soc. Am., 69(2), 264(Feb 1979).

A-3. "Laser Induced Damage in Optical Materials," Eds. A.I. Glass and A.H. Guenther, National Bureau of Standards (U.S.) Special Publication No. 509 (1977), p. 112.

That is, the causes of absorption as well as the amount of absorption must be learned. Infared spectroscopy allows one to scan a whole range of vibrational absorption bands, and to identify an individual absorber by its characteristic bands. External reflection allows the light to be manipulated so that more information may be obtained from the IR spectra. Multiplying the number of times a light beam is reflected from a film multiplies the absorptance of the light by the number of reflections, thereby greatly increasing the sensitivity. Data are easily reduced by techniques designed by Hansen (Ref. A-2).

The samples studied were three-phase systems; air, film, and metallic substrate (Fig. A-1). The equations which describe such systems for external reflection require only the initial phase to be transparent, while the second and third phases can be of any material. The third phase of each sample was a layer of silver which served as a mirror. The optical properties of the materials can be described by three optical constants: μ, the magnetic permeability which is 1 for all nonferromagnetic materials; n, the real index-of-refraction; and k, the extinction coefficient. The complex index-of-refraction $\hat{n} = n + ik$, and the complex dielectric constant is defined as $\hat{\varepsilon} = \hat{n} / \mu$. For dielectric materials, k=0 in regions of transparency.

The relationship between the reflected light and absorption within the film must be examined. As light passes into phase 2 of a three-phase system at angle-of-incidence θ, a standing wave is set up inside the second phase. This standing wave is described by the mean square of the electric field ($\langle E^2 \rangle$) (Ref. A-4). Absorption at a given point in any phase is proportional to the strength of the electric field of the light at that point (Ref. A-5). Knowing what the $\langle E^2 \rangle$ field profile is inside the film reveals where the absorption is taking place. The profile changes with varying wavelength, film thickness, and angle of incidence. Total absorptance $A_t = 1 - I/I_o$ after all reflections. I_o is the incident light and I the reflected.

Equations describing the position and magnitude of the field are extensive and will not be discussed here. They are developed fully in Reference A-6. Calculations involving these equations are usually done by computer.

If the third phase is a mirror, k_3 is very large, and the electric field penetrates the third phase only a few hundred angstroms. Thus, a 0.1 μm layer of some metal such as silver (Ag) can be assumed to have infinite thickness. In such a case, the x and y components of the field, $\langle E^2 \rangle_x$ and $\langle E^2 \rangle_y$ in Figure A-1, always have a node at the second interface

---

A-4. N.J. Harrick, Internal Reflection Spectroscopy, (Interscience, New York, 1967).

A-5. J.A. Stratton, Electromagnetic Theory, (McGraw-Hill, New York, 1941).

A-6. W.N. Hansen, J. Opt. Soc. Am., 58, 380 (1968).

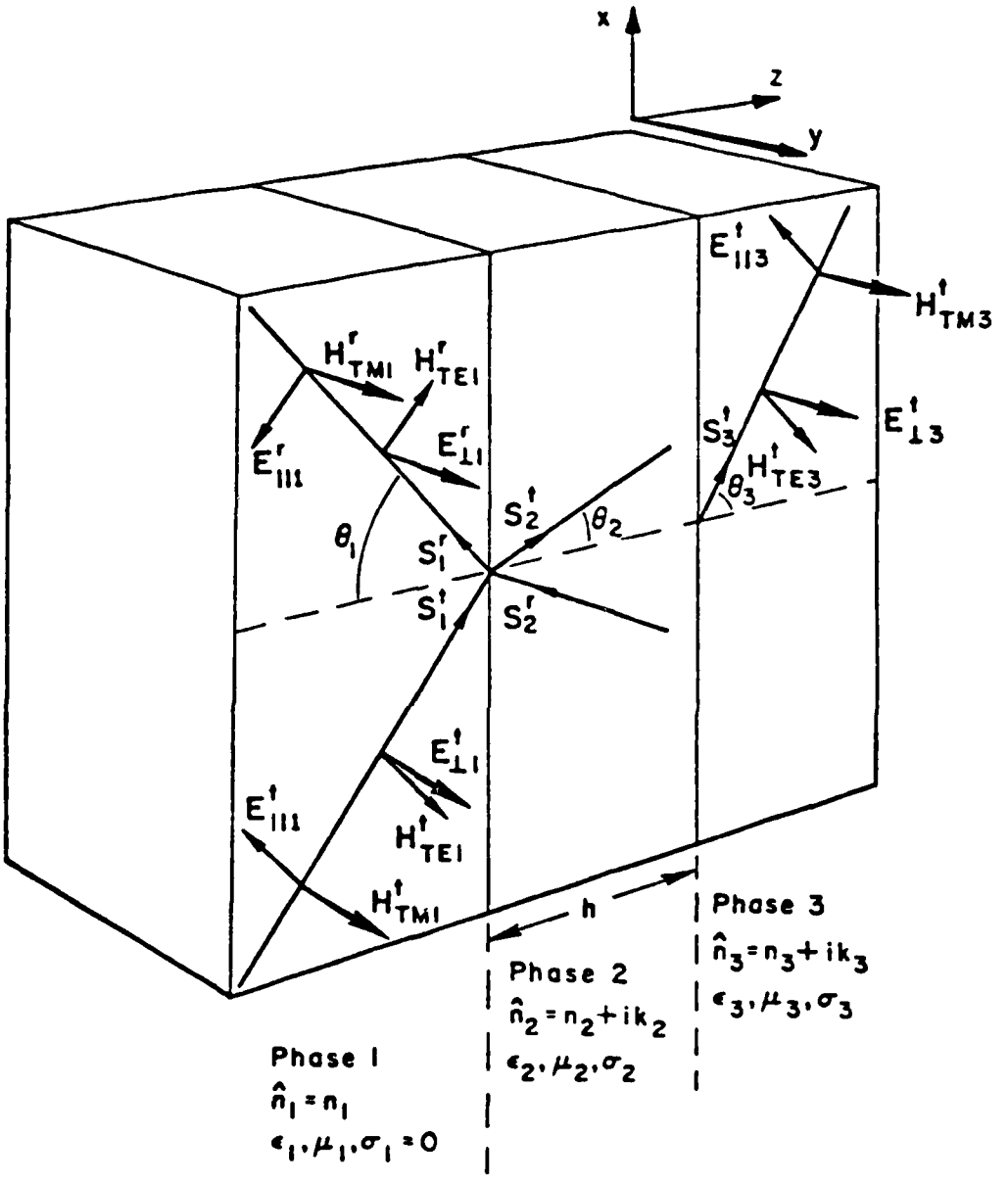

Figure A1. Interaction of plane wave in a three-phase system. Sign conventions for parallel (|| or TM) and perpendicular ($\perp$ or TE) polarized radiation. Zero phase change in all cases.

(film/mirror), while the z component, $\langle E^2\rangle_z$, always has a maximum at that interface; $\langle E^2\rangle_\perp = \langle E^2\rangle_y$, and $\langle E^2\rangle_\parallel = \langle E^2\rangle_x + \langle E^2\rangle_z$.

The equations for the reflection coefficient r at a plane boundary of two phases, j and k, are

$$r_{\perp jk} = \frac{\mu_k \xi_j - \mu_j \xi_k}{\mu_k \xi_j + \mu_j \xi_k}$$

$$r_{\parallel jk} = \frac{\frac{\xi_j}{\hat{\epsilon}_j} - \frac{\xi_k}{\hat{\epsilon}_k}}{\frac{\xi_i}{\hat{\epsilon}_j} + \frac{\xi_k}{\hat{\epsilon}_k}} \qquad \text{(A-1)}$$

$$\xi_j \equiv \hat{n}_j \cos\theta_j = (\hat{n}_j^{\,2} - n_1^{\,2}\sin^2\theta_1)^{1/2} \qquad \text{(A-2)}$$

$$\beta_j \equiv 2\pi h \xi_j / \lambda$$

$$R_\perp = |r_\perp|^2 \quad , \qquad R_\parallel = |r_\parallel|^2$$

The following real equations can be derived from the equations above.

$$R_\perp = \frac{(R_{\perp 12} + R_{\perp 23} e^{-4\mathrm{Im}\beta} + R_{\perp 12}^{\frac{1}{2}} R_{\perp 23}^{\frac{1}{2}} e^{-2\mathrm{Im}\beta} 2\cos(\delta^r_{\perp 23} - \delta^r_{\perp 12} + 2\mathrm{Re}\beta)}{(1 + R_{\perp 12} R_{\perp 23} e^{-4\mathrm{Im}\beta} + R_{\perp 12}^{\frac{1}{2}} R_{\perp 23}^{\frac{1}{2}} e^{-2\mathrm{Im}\beta} 2\cos(\delta^r_{\perp 12} + \delta^r_{\perp 23} + 2\mathrm{Re}\beta)} \qquad \text{(A-3)}$$

$$R_\parallel = \frac{(R_{\parallel 12} + R_{\parallel 23} e^{-4\mathrm{Im}\beta} + R_{\parallel 12}^{\frac{1}{2}} R_{\parallel 23}^{\frac{1}{2}} e^{-2\mathrm{Im}\beta} 2\cos(\delta^r_{\parallel 23} - \delta^r_{\parallel 12} + 2\mathrm{Re}\beta)}{(1 + R_{\parallel 12} R_{\parallel 23} e^{-4\mathrm{Im}\beta} + R_{\parallel 12}^{\frac{1}{2}} R_{\parallel 23}^{\frac{1}{2}} e^{-2\mathrm{Im}\beta} 2\cos(\delta^r_{\parallel 23} + \delta^r_{\parallel 12} + 2\mathrm{Re}\beta)} \qquad \text{(A-4)}$$

The angle of incidence is θ, and the thickness of the second phase is h although the dimensionless h/λ will be used for convenience.

The phase shift δ^r of the reflected light at each interface is defined as the argument of the reflection coefficient.

$$\delta^r = \arg r \qquad \text{(A-5)}$$

If phases j and k are dielectrics, then at the interface of the two dielectrics the external-reflection phase change will always be 180 degrees for perp polarization. For par polarization, the phase external-reflection change will be 0 degree for $\theta = 0$ degree becoming 180 degrees at Brewster's angle.

$$\delta_{\perp}^{r} = 180^{o}, \text{ all } \theta$$

$$\delta_{\parallel}^{r} = 0^{o}, \theta = 0$$

$$\delta_{\parallel}^{r} = 180^{o}, \theta \gtrsim \theta_{B}$$

At $\theta = 0^{o}$, $\langle E^{2} \rangle$ has no z component, and absorption at the second interface will not occur. At oblique θ, absorptions at that interface will show up.

II. EXPERIMENTAL

1. SPECTROSCOPY

This research required a setup in which the IR light beam could be reflected externally from a film, several times at oblique θ, or a single time at normal incidence, before entering the monochromator. The films were studied using external reflection techniques with Perkin Elmer (PE) 180 and 621 spectrophotometers, along with specially-designed attachments. A diagram of the arrangement of the sample (on a microscope slide) inside the PE 180 spectrometer for oblique angles, external reflection is shown in Figure A-2. The number of reflections were counted by looking through the sample with mirrors and counting the number of edges where the sample slide touches the sample mount. Many of the spectra were taken using a gold grating polarizer inside the PE-180. Spectra were run from 4000 cm^{-1} to approximately 400 cm^{-1} with the PE-621, and from 4000 cm^{-1} to 180 cm^{-1} with the PE-180, which is the better of the two instruments.

The samples studied were prepared by evaporation techniques at the Air Force Weapons Laboratory (AFWL) at Kirtland Air Force Base, New Mexico. The ZnS and ThF_4 films were studied because of their common usage in laser optics. Molybdenum disks (used with the normal incidence, single reflection method) and microscope slides (used with the oblique, θ, multiple-reflection method) were first coated with a 0.2 μm layer of Ag. To some was added a very thin (100-200 Å) layer of SiO, and the ZnS or ThF_4 films were layed on top. The thickness of the SiO layer was insignificant, and was treated only as an impurity at the second interface. It served as a reference with its vibrational absorption band at 1130 cm^{-1}. Table A-1 gives a description of different samples, and Table A-2 gives the thickness of a few of the films as determined by the Tally step (an instrument which uses a tiny diamond probe to mechanically measure the thickness of a film) and by determination methods discussed later.

Samples were analyzed by scanning the net $R = I/I_o$ versus wavelength and examining the absorption bands to determine the cause of each absorption.

2. COMPUTER ANALYSIS

Using the UNIVAC computer at NWC, calculations were made of the location and magnitude of the various components of $\langle E^2 \rangle$, as well as the corresponding values of $R_{\text{per and par}}$ and $\delta_{\text{per and par}}$. (Here δ is the total phase change of the system, not of each boundary.) R, δ, and $\langle E^2 \rangle$ were calculated as functions of h/λ, depth within the second phase (z/λ), and θ, respectively. Parameters for the calculations included n_1, n_2, and n_3 and k_3 taken from literature. The corresponding equations are found in Reference A-6 as mentioned before, and the computer program was written and compiled by Hansen and co-workers at Utah State University. Results are found in Tables A-3 through A-5.

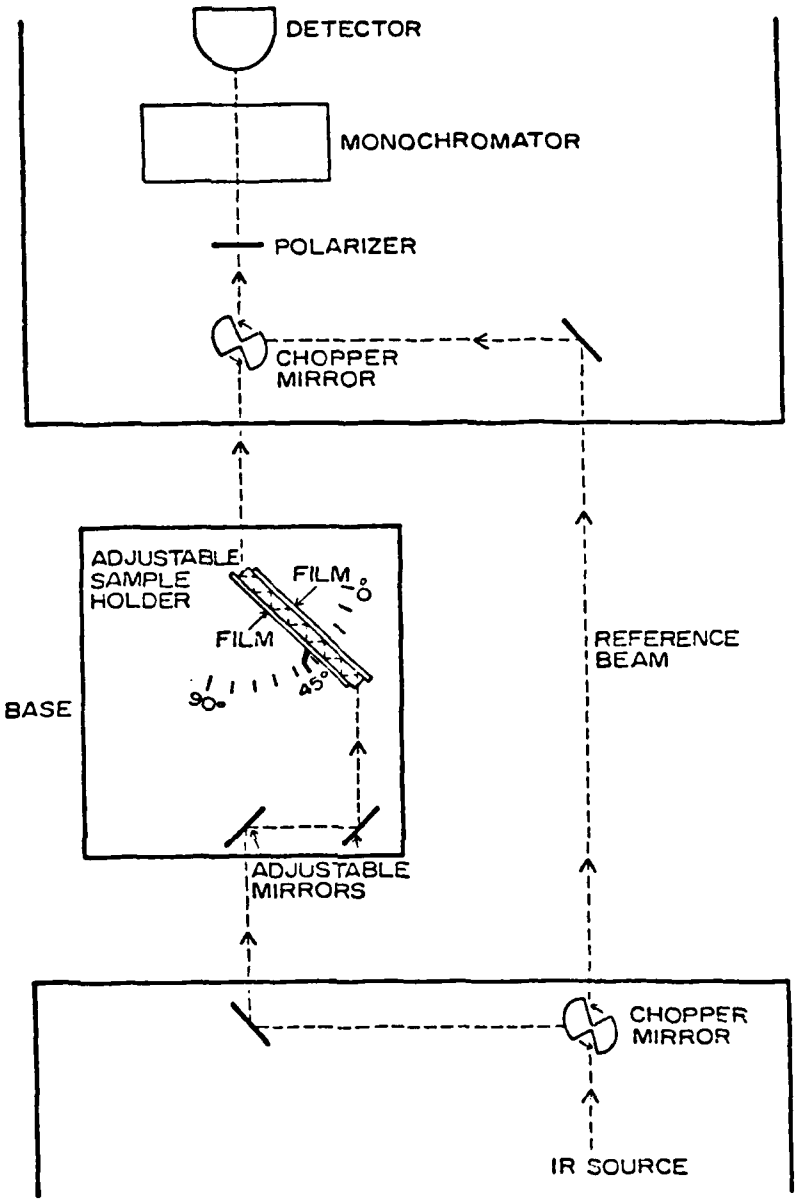

Figure A2. External reflection setup inside of PE 180 spectrophotometer. Two microscopes slide samples used.

TABLE A1. DESCRIPTION OF SAMPLES

Sample #	Type	100Å SiO
2-A	ZnS	No
2-B	ZnS	Yes
4-A	ThF_4	No
4-B	ThF_4	Yes

Thicknesses of the ZnS films will vary somewhat, as will the thicknesses of the ThF_4 films.

Samples made at AFWL, Kirtland AFB, NM.

TABLE A2. TALLY STEP DETERMINATION OF THICKNESS

Sample #	Polarization	θ	# of Reflections	Tally Step	Calc.h+ (μm)
$2\text{-}B_1$	par	45°	13	---	0.815 μm
$2\text{-}B_2$	perp	45°	13	0.820μm±20Å	0.813 μm
$4\text{-}B_2$	perp	45°	13	2.62μm±30Å	2.28 μm
$4\text{-}B_1$	par	0°	1	---	2.27 μm

Samples $2\text{-}B_1$ and $2\text{-}B_2$ were made at the same time, as were $4\text{-}B_1$ amd $4\text{-}B_2$. However, thickness of their films may vary slightly.

Tally Step used at NWC, China Lake, CA.

+From the equation $h/\lambda = (2n+1)/4\xi \quad \xi = (\hat{n}-n_1^2\sin^2\theta_1)^{1/2}$

TABLE A3. ELECTRIC FIELD INTENSITY CALCULATIONS

h/lamda	$\langle E^2 \rangle_{per}$	$\langle E^2 \rangle_{par}$	R_{per}	δ_{per}	R_{par}	δ_{par}
0.000	0.352 -03	0.703 -03	0.9967	-178.9	0.9934	+2.144
0.010	0.117 -01	0.104 +00	0.9966	-173.8	0.9933	11.34
0.020	0.404 -01	0.147 +00	0.9965	-168.5	0.9931	20.78
0.030	0.898 -01	0.219 +00	0.9961	-162.8	0.9927	30.68
0.040	0.166 +00	0.322 +00	0.9957	-156.4	0.9921	41.30
0.050	0.282 +00	0.463 +00	0.9949	-149.2	0.9912	52.90
0.060	0.454 +00	0.648 +00	0.9938	-140.5	0.9902	65.83
0.070	0.717 +00	0.879 +00	0.9922	-129.8	0.9888	80.45
0.080	0.112 +01	0.115 +01	0.9896	-115.8	0.9872	97.15
0.090	0.175 +01	0.146 +01	0.9857	-97.81	0.9855	116.2
0.100	0.265 +01	0.174 +01	0.9800	-70.23	0.9838	137.7
0.110	0.361 +01	0.193 +01	0.9739	-34.00	0.9827	161.2
0.120	0.392 +01	0.198 +01	0.9720	+9.268	0.9824	-174.2
0.130	0.324 +01	0.186 +01	0.9763	50.41	0.9831	-150.0
0.140	0.224 +01	0.161 +01	0.9826	82.50	0.9846	-127.4
0.150	0.145 +01	0.131 +01	0.9875	105.6	0.9863	-107.0
0.160	0.931 +00	0.102 +01	0.9908	122.2	0.9880	-89.04
0.170	0.593 +00	0.765 +00	0.9930	134.6	0.9895	-73.36
0.180	0.373 +00	0.555 +00	0.9944	144.4	0.9907	-59.58
0.190	0.228 +00	0.392 +00	0.9953	152.4	0.9917	47.32
0.200	0.130 +00	0.269 +00	0.9959	159.2	0.9924	36.21
0.210	0.661 -01	0.181 +00	0.9963	165.2	0.9929	25.97
0.220	0.260 -01	0.123 +00	0.9966	170.7	0.9932	-16.31
0.230	0.495 -02	0.922 -01	0.9967	176.0	0.9934	-7.009
0.240	0.350 -03	0.858 -01	0.9967	-176.0	0.9934	+2.137
0.250	0.117 -01	0.104 +00	0.9966	-173.8	0.9933	11.33
0.260	0.403 -01	0.147 +00	0.9965	-168.5	0.9931	20.77

$n_1 = 1.00$
$n_2 = 2.20$
$n_3 = 6.60$ $k_3 = 75.0$ $\theta = 45.0^{o}$

$\langle E^2 \rangle$ is at 1st interface (z/lamda = 0.0)

δ_{per} and δ_{par} are the total phase changes, not for each interface independently.

NOTE: As the thickness h/λ changes, $\langle E^2 \rangle$, R, and δ pass through maxima and minima.

TABLE A4. ELECTRIC FIELD INTENSITY CALCULATIONS

θ^o	h/lamda	$\langle E^2 \rangle_{per}$	$\langle E^2 \rangle_{par}$	R_{per}	R_{par}
0.0	0.1249	3.99996	3.99996	0.999988	0.999988
45.0	0.1335	3.99995	1.99998	0.999985	0.999990
50.0	0.1352	3.9999	1.6522	0.999984	0.999991
55.0	0.1369	3.9999	1.3165	0.999983	0.999992
60.0	0.1387	3.9998	1.000	0.999981	0.999993
65.0	0.1402	3.9998	0.7145	0.999977	0.999994

$n_1 = 1.00$
$n_2 = 2.00$
$n_3 = 3.00$ $\quad k_3 = 2000$

h/lamda = thickness of film a min R (minimum reflectance)

$\langle E^2 \rangle$ is at 1st interface ($z/\lambda = 0.0$)

R_{per} and R_{par} = min R_{per} and min R_{par} at the h/lamda and θ

NOTE: Here, k_3 =2000 was used to see what happens at k when it is very large. It does not effect the location of min R, but increases the total reflectance.

TABLE A5. ELECTROID FIELD INTENSITY CALCULATIONS

h/lamda	$\langle E^2 \rangle_{per}$	$\langle E^2 \rangle_{par}$	R_{per}	δ_{per}	R_{per}	δ_{par}
0.1960	3.9658	1.98897	0.98811	-5.8454	0.989258	+178.46
0.1965	3.9683	1.98912	0.98811	-5.1032	0.989258	178.96
0.1970	3.9704	1.98920	0.98811	-4.3608	0.989258	179.46
0.1975	3.9722	1.98924	0.98810	-3.6180	0.989258	179.95
0.1980	3.9736	1.98921	0.98810	-2.8751	0.989258	-179.55
0.1985	3.9748	1.98914	0.98810	-2.1320	0.989258	-179.05
0.1990	3.9756	1.98900	0.988095	-1.3888	0.989259	-178.55
0.1995	3.9760	1.9888	0.988094	-0.6455	0.98926	-178.05
0.2000	3.9761	1.9886	0.988094	+0.0776	0.98926	-177.55
0.2005	3.9759	1.9883	0.988094	0.8411	0.98926	-177.05

$n_1 = 1.00$
$n_2 = 1.40$
$n_3 = 0.757$ $k_3 = 22.786$ $\theta = 45.0^{\circ}$

$\langle E^2 \rangle$ is at 1st interface (z/lamda = 0.0)

δ_{per} and δ_{par} are the total phase change

NOTE: This table shows that at oblique θ, h/λ for min R_{per} is shifted slightly from h/λ for min R_{par}.

III. RESULTS

1. H_2O AND C-H

The most obvious and first-noticed absorption bands on the IR spectrum of ThF_4 are due to large amounts of H_2O (Figs. A-3 and A-4). Finding such prominent bands of water, even with a single reflection, was surprising. These bands are found at 3500 cm^{-1}, 1620 cm^{-1}, and 530 cm^{-1}.

The water proved to be inside the film and not on one of its surfaces. The $\langle E^2 \rangle_{x\&y}$ fields were found to have nodes at both interfaces, with maximum field strength inside the film. In at attempt to drive off the water, one sample, 4-B_2, was heated to 280°C. Although part of the film chipped off as a result of rapid cooling, IR showed that the same amount of H_2O remained within the film. Spectra were then taken of some samples of ThF_4 on Ag which had been capped with a ZnSe layer immediately after deposition. As is seen in Figures A-5 through A-8, large amounts of water still are present.

The absorption due to water occurs at the wavelengths of the HF, DF, CO_2, and other important lasers. Getting rid of the water is evidently an important problem yet to be solved.

2. INTERFERENCE BAND

As the spectra of ZnS were being taken, an unexpected absorption pattern emerged (Figs. A-9 and A-10). There is no evidence of H_2O or C-H as in ThF_4, and ZnS itself has absorption bands only at 350 cm^{-1} and 265 cm^{-1}. In Figure A-9 ZnS has two absorption peaks; at 350 cm^{-1} and 265 cm^{-1}. However, in Figure A-10 only the 265 cm^{-1} peak shows up. This is because the absorption at 350 cm^{-1} is due to a longitudinal wave excitation called a polariton. This is seen only with par polarization. Yet there is a long smooth periodic absorption band with minimum reflectance (min R) around 1450 cm^{-1}. The spectrum is broad at max R while sloping to a peak at min R. At min R, the absorptance $A_1 \sim 0.03$ per reflection at normal incidence.

This same band is found in the ThF_4 film spectra (Figs. A-3 and A-4). Min R is at 730 cm^{-1} and 2220 cm^{-1} at $\theta = 0$ deg, and at 740 cm^{-1} and 2400 cm^{-1} at $\theta = 45$ deg. These minima are difficult to detect from among the other large bands of H_2O and ThF_4. Yet this interference band is also regular and periodic. The bands in the ZnSe-capped ThF_4 films (Figs. A-5 through A-8) are especially large.

This absorption band in ZnS and ThF_4 cannot be due to impurities or scattering centers. The band is seen to be periodic in wave number, and Figures A-5 through A-8 show that the absorption peaks shift from one wave number to another with $\Delta\theta$. At the same time, the H_2O and SiO peaks (SiO at 1140 cm^{-1}) do not move. Therefore, the bands are not due to any vibrational mode absorption. Neither are they caused by light scattering. Were this the case, the reflectance would not be periodic and would not shift in the way observed. Also, the H_2O and SiO peaks would be affected.

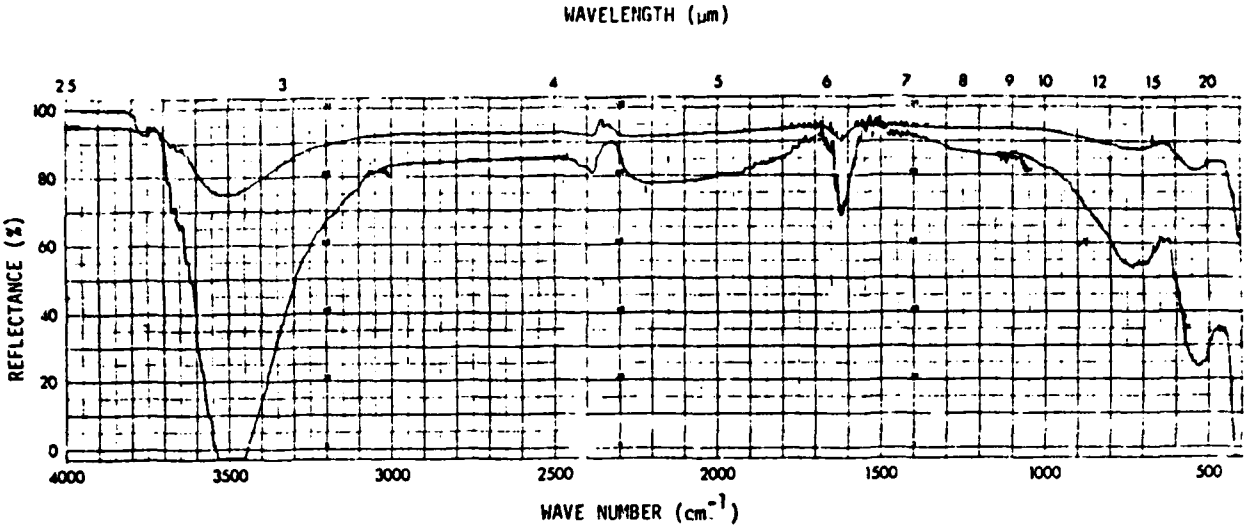

Figure A3. Sample 4-B_2. θ = 0 deg, parallel polarized. One reflection. First min R -735 cm^{-1}, second min R - 2220 cm^{-1}.

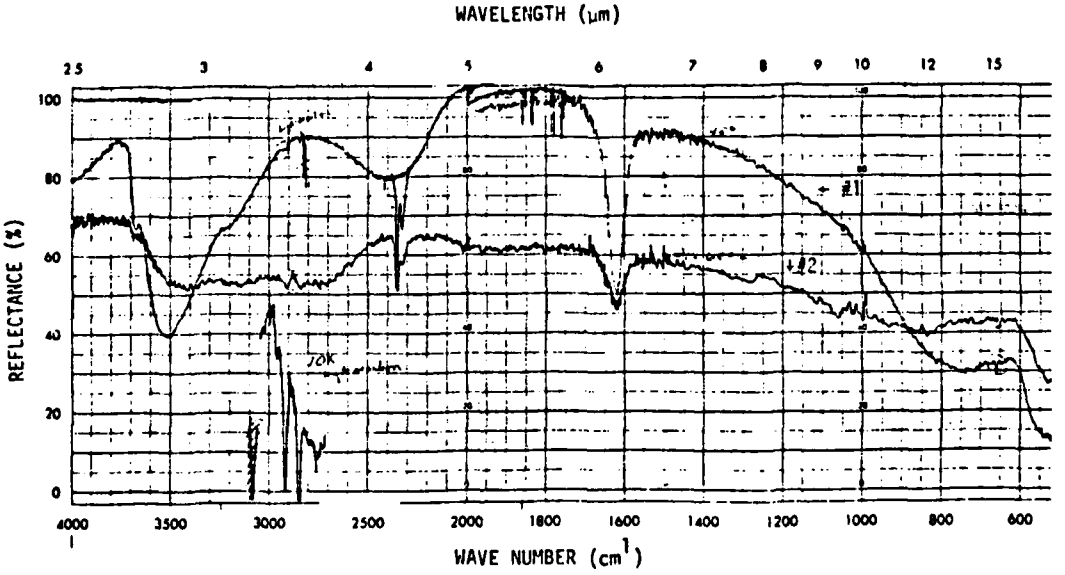

Figure A4. Sample 4-B_1. θ = 45 deg perp polarized, 13 reflections. First min R -745 cm^{-1}, second min R - 2400 cm^{-1}.

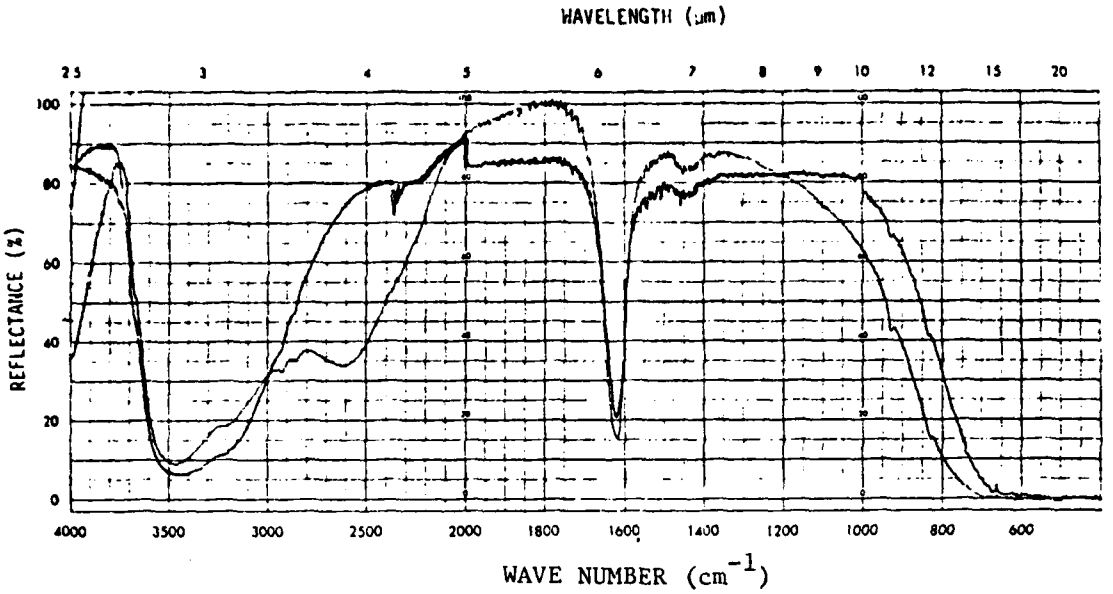

Figure A5. Thorium fluoride on silver with zinc selenide cap; θ_1 = 45 deg, θ_2 = 67 deg, at Brewster's angle there is no par light reflected from the first interface. Consequently, this figure shows no interference at 67 deg.

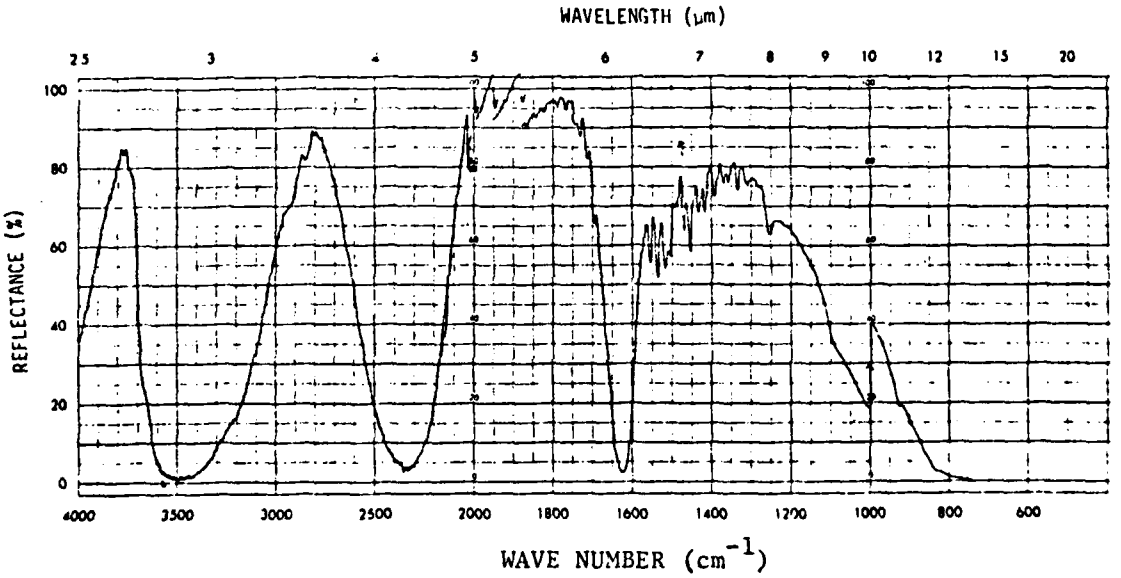

Figure A6. Thorium fluoride on silver with zinc selenide cap; θ = 0 deg, parallel polarized with many reflections (second min R - 2345 cm^{-1}).

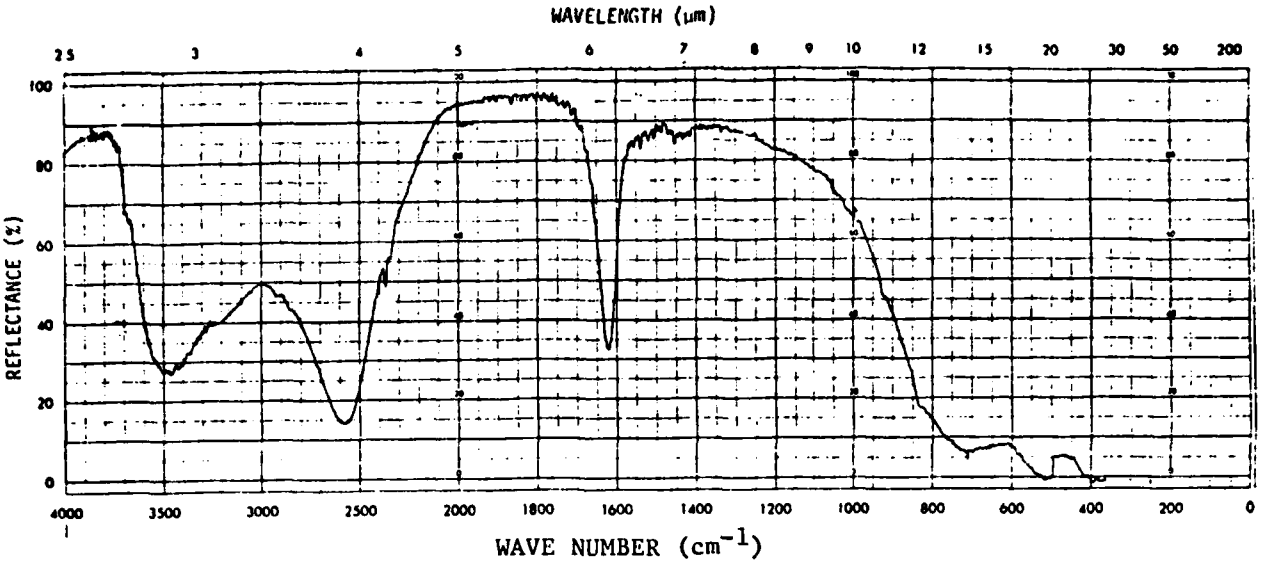

Figure A7. Thorium fluoride on silver with zinc selenide, θ = 45 deg, perp polarization, 24 reflections (second min R - 2585 cm^{-1}). C-H peak at 2840 cm^{-1} and 2930 cm^{-1}.

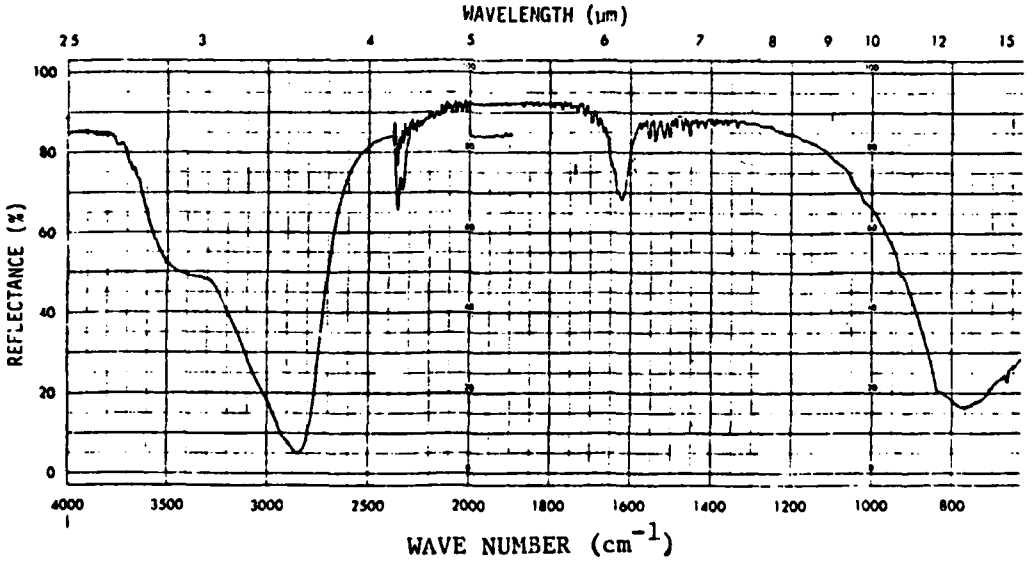

Figure A8. Thorium fluoride on silver with zinc selenide cap; θ = 67 deg, perp polarization, 10 reflections (first min R - 770 cm^{-1}; second min R - 2850 cm^{-1}). C-H bands present and enlarged at 2860 cm^{-1} and 2925 cm^{-1}.

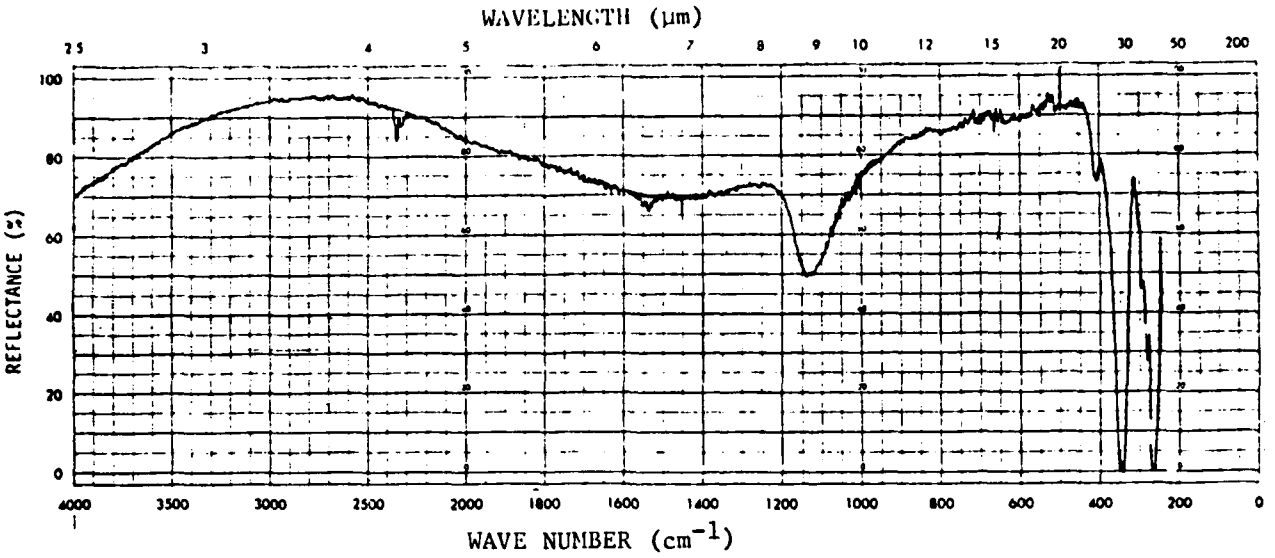

Figure A9. Sample 2-B, θ = 45 deg, parallel polarization, 13 reflections (first min R - 1450 cm^{-1}).
Note: Silicon monoxide at 1130 cm^{-1}.

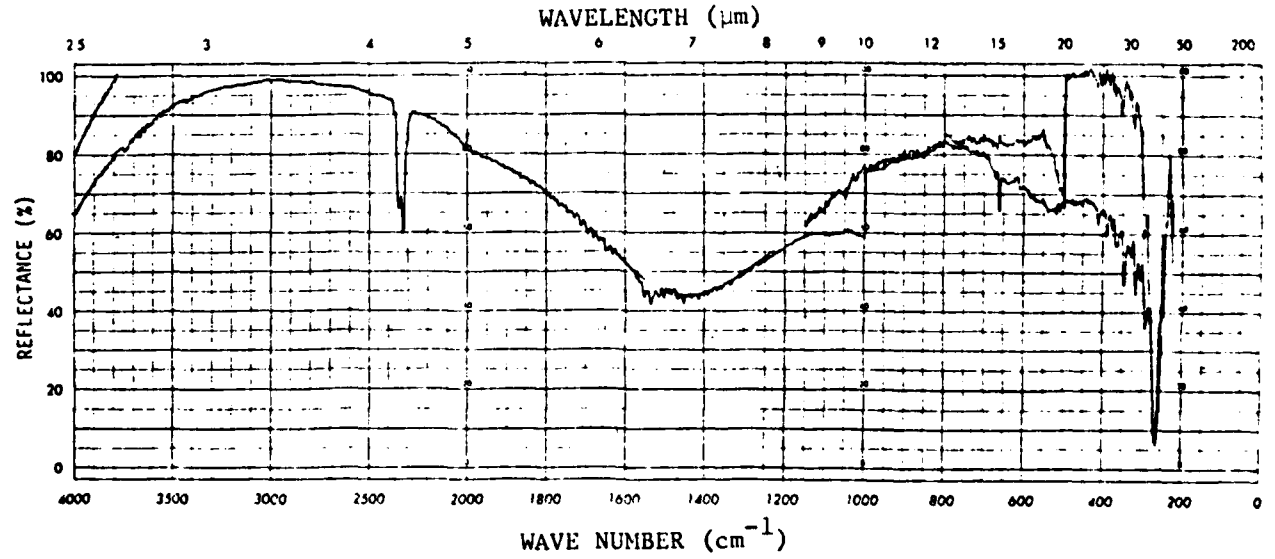

Figure A10. Sample 2-B_2, θ = 45 deg, perp polarization, 13 reflections (first min R - 1450 cm^{-1}). Note that there is no peak at 345 cm^{-1}.

Close examination of the samples themselves showed no appreciable scattering of light.

The absorption must be due to interference inside the film, causing periodic high absorption in the silver substrate. That is, part of the light which is reflected off of the Ag surface after passing through the dielectric material interferes destructively with the 5% of the initial light beam which is reflected off of the dielectric surface. The energy which is not reflected due to interference must be absorbed by the silver substrate, which may cause extensive damage to optical components. If this is really the cause of the absorption band, then this absorption will occur even if the film is absolutely perfect. This reduction in reflectance is quite unacceptable, much greater than the 10^{-4} guideline mentioned before.

3. COMPUTER ANALYSIS

To better understand the behavior of this interference absorption, calculations were made by computer of $\langle E^2 \rangle_{\text{per \& par}}$, $R_{\text{per \& par}}$ and $\delta_{\text{per \& par}}$ as functions of h/λ, z/λ, and θ, respectively. The analysis verified the fact that the absorption band is due to interference. Some very interesting results were found.

(1) Min $R_\perp$ occurs at each h/λ where $\langle E^2 \rangle_\perp$ is maximum at the first interface (air/film). Max $R_\perp$ occurs at each h/λ where $\langle E^2 \rangle_\perp$ has a node at the first interface (Table A-3). Although opposite, $R_\perp$ and $\langle E^2 \rangle_\perp$ are symmetrical, i.e., both are sharp or broad at the same h/λ (Figs. A-11 and A-12). The same is true for $R_{||}$ and $\langle E^2 \rangle_{||}$.

(2) The thickness h/λ for min $R_\perp$ changes as θ changes. That is, for a given h, λ at min $R_\perp$ shifts. Results show that h/λ increases as θ increases (Table A-4).

(3) Close analysis shows that min $R_\perp$ shifts a little from min $R_{||}$ at oblique θ. Also, max $R_\perp$ > max $R_{||}$, while $R_\perp$ < min $R_{||}$ at oblique θ. At $\theta = 0$, $R_\perp$ and $R_{||}$ are indistinguishable (Table A-5).

(4) Calculations show that $\langle E^2 \rangle_\perp$ at the second interface is over six times greater at min $R_\perp$ than at max $R_\perp$. This means that when a min $R_\perp$ occurs, the node at the film/Ag interface is not really a node, and energy is dissipated into the Ag.

(5) The greater the k value, the closer R min or max is to 1.

(6) At min $R_\perp$ and $R_{||}$, $\delta = 0$ deg and $\delta_{||} = 180$ deg (+→-). At max $R_\perp$ and $R_{||}$, $\delta_\perp = 180$ deg (+→--), and $\delta_{||} = 0$ deg (Table A-3).

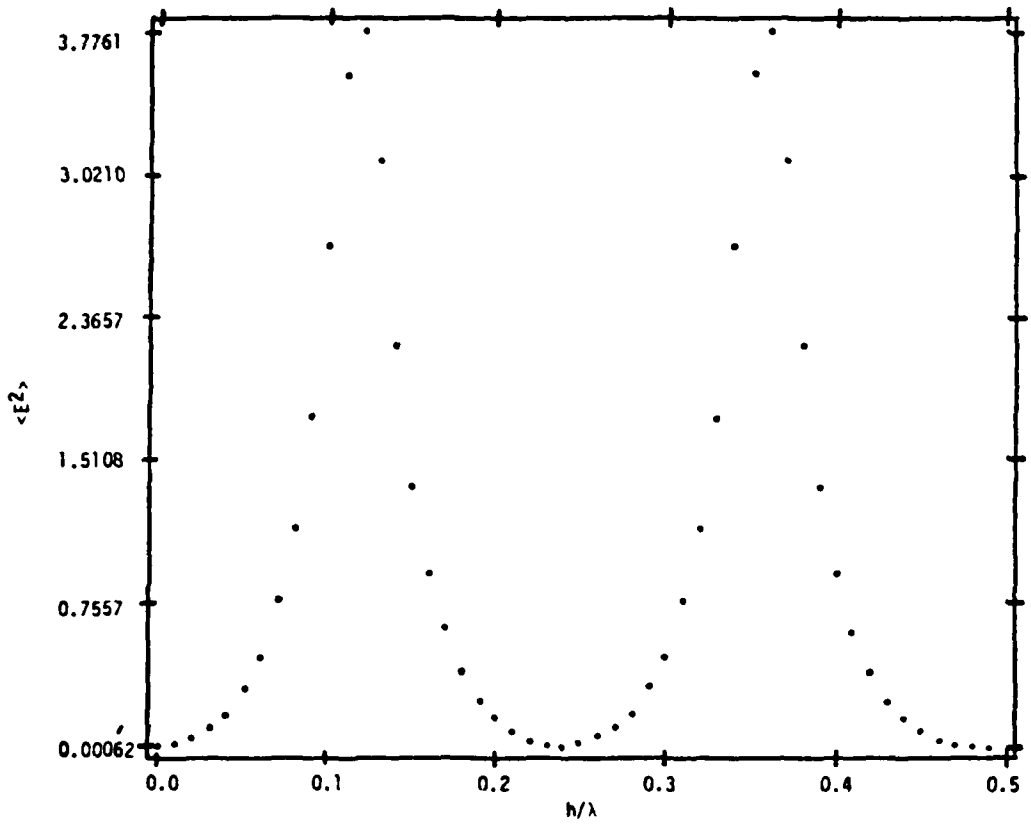

Figure A11. $\langle E^2 \rangle$ versus h/λ. The sample is ZnS on Ag with θ, being 45.0 deg and λ set at 10 μm. ($n_1 = 1.0$, $n_2 = 2.0$, $n_3 = 4.5$, and $k_3 = 55.2$.)

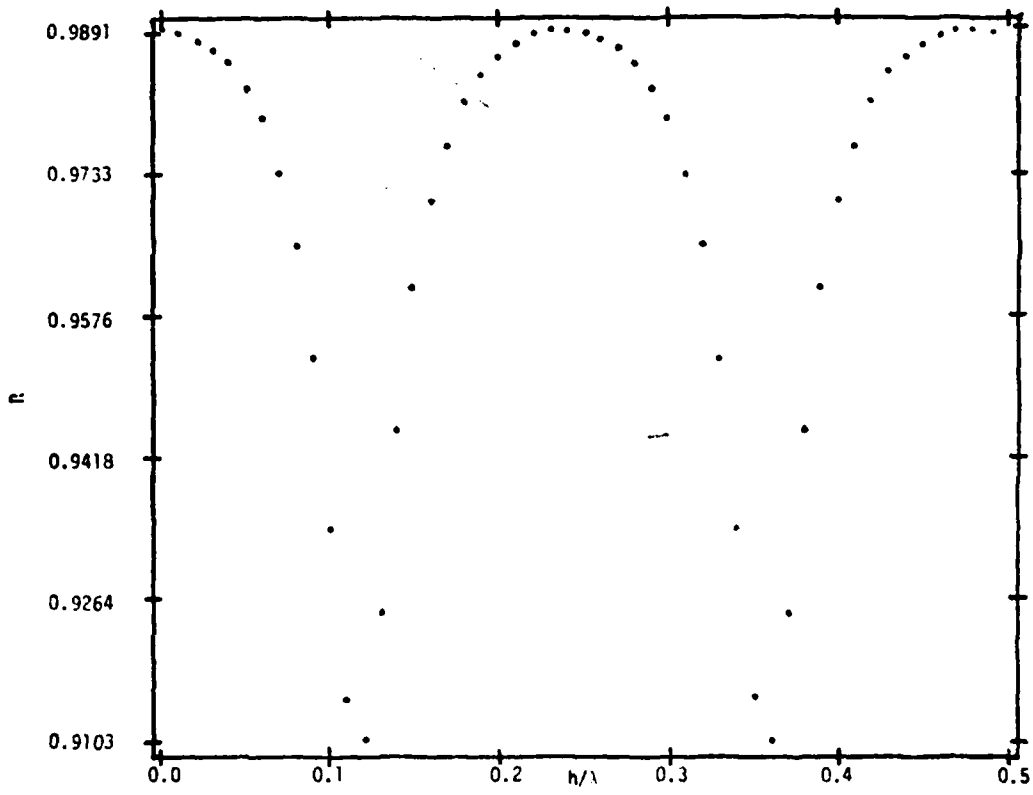

Figure A12. R versus h/λ for ZnS on Ag. The conditions are the same as in Figure A11.

IV. DERIVATION OF ANOMALOUS INTERFERENCE EQUATION

Whether or not a min R will occur in a given film depends on h, λ, θ, and $\hat{n}$. It is essential to be able to predict when a min R or max R will occur so that the conditions can be varied as needed. A fundamental equation which describes the behavior of the interference absorption inside the same could be important in thin film analysis. Also, it is difficult to calculate by computer values for h/λ at min R because the index-of-refraction $\hat{n}$ for both the film and Ag changes as λ changes.

Such an equation is derived from Equations A-3 and A-4. This is done by taking the derivative of R with respect to h, holding λ and ξ constant, and setting the derivative equal to zero, thus finding the critical points of reflectance.

Setting $\mathrm{Im}\beta = 0$ (β for second phase),

$$(\delta^r_{\perp 23}+\delta^r_{\perp 12}+2\mathrm{Re}\beta) = (+) \quad \text{and} \quad (\delta^r_{\perp 23}-\delta^r_{\perp 12}+2\mathrm{Re}\beta) = (-)$$

$$(1+R_{\perp 12}R_{\perp 23}+R^{1/2}_{\perp\ 12}R^{1/2}_{\perp\ 23}2\cos(+))(-R^{1/2}_{\perp\ 12}R^{1/2}_{\perp\ 23}4\sin(-))2\pi\xi/\lambda$$

$$\frac{dR_\perp}{dh} = \frac{-(R_{\perp 12}+R_{\perp 23}+R^{1/2}_{\perp\ 12}R^{1/2}_{\perp\ 23}2\cos(-))(-R^{1/2}_{\perp\ 12}R^{1/2}_{\perp\ 23}4\sin(+))2\pi\xi/\lambda}{(1+R_{\perp 12}R_{\perp 23}+R^{1/2}_{\perp\ 12}R^{1/2}_{\perp\ 23}2\cos(+))^2}$$

Setting the numerator equal to 0, and multiplying through,

$$\sin(-) + R_{\perp 12}R_{\perp 23}\sin(-) + R^{1/2}_{\perp\ 12}R^{1/2}_{\perp\ 23}2(\cos(+)\sin(-) - \cos(-)\sin(+))$$

$$- R_{\perp 12}\sin(+) - R_{\perp 23}\sin(+) = 0$$

Noting that $\cos(+)\sin(-) - \cos(-)\sin(+) = 0$ and

$$\sin(+) = \sin(-)$$

when

$$\delta^r_{\perp 12} = 180^0 \quad (\hat{n} = n \text{ for dielectric}) \text{ from Equation 5}$$

then

$$\sin(\delta^r_{\perp 23} \pm 180^0 + 2\mathrm{Re}\beta)(1 + R_{\perp 12}R_{\perp 23} - R_{\perp 12} - R_{\perp 23}) = 0$$

Since

$$(1+R_{\perp 12}R_{\perp 23}-R_{\perp 12}-R_{\perp 23}) = (R_{\perp 12}-1)(R_{\perp 23}-1) \neq 0$$

because $R_{12} \neq 1$ and $R_{23} \neq 1$, therefore,

$$\sin(\delta^{r}_{\perp 23} \pm 180^{o} + 2Re\beta) = 0$$

and

$$\delta^{r}_{\perp 23} \pm 180^{o} + 4\pi h\xi/\lambda = 0, \pi, 2\pi, \ldots n\pi$$

The values for h/λ at max R and min R are

$$h/\lambda = (n - (\delta^{r}_{\perp 23} \pm 180^{o})/180^{o})/4\xi_j \quad \xi_j = (\hat{n}_j^2 - n_1^2 \sin^2\theta_j)^{1/2} \qquad (A\text{-}6)$$

$$n = 0, 1, 2, 3, \ldots\infty$$

To find which values for h/λ are at max R and which are at min R substitute either $2n/4\xi$ or $(2n+1)/4\xi$ back into Equation A-3 (assume $\delta_{23} = 180^{o}$). As a result,

$$\frac{(2n+1)/4\xi}{(1+R_{\perp 12}R_{\perp 23}-2R^{1/2}_{\perp 12}R^{1/2}_{\perp 23})} \;?\; \frac{2n/4\xi}{(R_{\perp 12}+R_{\perp 23}-2R^{1/2}_{\perp 12}R^{1/2}_{\perp 23})} \quad < \quad \frac{(1+R_{\perp 12}R_{\perp 23}+2R^{1/2}_{\perp 12}R^{1/2}_{\perp 23})}{(R_{\perp 12}+R_{\perp 23}+2R^{1/2}_{\perp 12}R^{1/2}_{\perp 23})}$$

With some manipulation,

$$(R^{1/2}_{\perp 12}R^{1/2}_{\perp 23}-1)^2(R^{1/2}_{\perp 12}+R^{1/2}_{\perp 23}) \;?\; < (R^{1/2}_{\perp 12}-R^{1/2}_{\perp 23})^2(R^{1/2}_{\perp 12}R^{1/2}_{\perp 23}+1)^2$$

Finally,

$$R_{\perp}^{1/2}{}_{12}R_{\perp 23} < R_{\perp}^{1/2}{}_{12}$$

because $R_{23} < 1$ always. Therefore, min R occurs at $(2n+1)/4\xi$ while max R occurs at $n/4\xi$.

It can also be shown that $R_{\perp}$ and $\frac{dR}{dh}_{\perp}$ are always defined for any value h/λ. Because R_{12} and R_{23} are always positive, the most negative value possible for the denominator is

$$1 + R_{\perp 12}R_{\perp 23} - 2R_{\perp}^{1/2}{}_{12}R_{\perp}^{1/2}{}_{23} = a$$

and

$$(R_{\perp}^{1/2}{}_{12}R_{\perp}^{1/2}{}_{23} - 1)^2 = a > 0 \text{ always}$$

These derived equations and proofs can also be applied to $R_{\parallel}$ as well. The resulting equations will look exactly the same except for $R_{\parallel}$ and $\xi_{\parallel}$ instead of $R_{\perp}$ and $\xi_{\perp}$.

V. SPECTRAL ANALYSIS OF INTERFERENCE BAND

1. COMPARISON

The equation describing the interference band is

$$h/\lambda = n/4\xi - (\xi^{r}_{23}-180^{o})/4\pi\xi \tag{A-7}$$

$$\text{Min R at } h/\lambda = (2n+1)/4\xi - (\xi^{r}_{23}-180^{o})/4\pi\xi \tag{A-8}$$

$$\text{Max R at } h/\lambda = (2n)/4\xi - (\xi^{r}_{23}-180^{o})/4\pi\xi \tag{A-9}$$

$$n = 0,1,2,3\ldots,\infty$$

Given certain parameters the behavior of the interference band can be described, calculating λ where min R or max R occur for a given film (given h, n, and θ), or calculating h for a given λ. Conversely, the different spectra can be used to find λ at which a min R occurs and thus calculate h of the film if n_2 is known, or n_2 if h is known. Table A-2 contains the results of thickness determinations by Tally step and by our method using the spectra. The two methods produce very similar results. This however cannot yet be done with the ZnSe-covered samples because of the fourth phase. This type of analysis using the interference phenomena has never been done before, and its usefulness is very apparent.

Inconsistencies in the distance between min R exist because n_2 and $\hat{n}_3$ are changing with $\Delta\lambda$. This is overcome by calculating each min R separately at its corresponding λ, n_2, and $\hat{n}_3$. Also, a good first approximation of Equation A-6 is made by assuming $\delta^{r}_{23} = 180$ deg. It is actually around 175 deg, but the difference in the results of the equation are slight, though noticeable. This helps account for the difference between consecutive min R.

Comparing the computer data with the spectra shows that the electric field theory accounts for the interference band, from which this equation is derived. The smooth periodic nature of the band, seen on the spectra, is predicted by the computer calculations. The ThF_4/ZnSe-capped samples show a shift in min R as θ changes, and also a small difference in the location of max and min R. However, the computer is much harder to work with, and programs are not available which take into account changes in $\hat{n}$.

2. ANOTHER TECHNIQUE FOR ANALYSIS

Close examination of the spectra of ThF_4 reveals an important technique of analysis. If a min R occurs close to an impurity band as shown in Figures A-5 and A-8, that band will be enhanced if the impurity is located on the first interface. This is because $\langle E^2 \rangle$ is at a maximum at

the first interface when there is minimum reflectance. If the band is not enhanced, it must be inside the film. Figures A-5 through A-8 show that the hydrocarbon is at the air/film interface. The same reasoning can be applied at the second interface. If at oblique θ an absorption occurs with parallel light but not with perpendicular polarized light, the impurity must be at the film/mirror interface where $\langle E^2 \rangle_{X\&Y}$ have a node. This is true of the SiO band at 1140 cm^{-1}, which is seen in Figure A-9 but not in Figure A-10. So, by changing θ and the polarization, fine-tuned analysis can be done with the samples to determine the location and type of absorbing species.

VI. CONCLUSIONS

Absorption due to interference is a surprising feature of external reflection from thin films. Under the right conditions (which from the results of this research is quite probable) extensive damage to the optical components of high-power lasers could result from the absorption of light into the silver. This has nothing to do with the quality of the film, and must be understood so that conditions can be properly altered. The equation $h/\lambda = n/4\xi$ describes the reflectance of this interference band and allows for the calculation of h/λ at maximum and minimum reflectance. Also, the optical constants of the film can be calculated if h is known from some other source such as Tally step.

The interference band can also be used as an analytical tool. The wavelength at which the reflectance is at a minimum changes with θ and allows the min R to be placed at a desired wavelength. When reflectance is at a minimum, $\langle E^2 \rangle$ is at a maximum at the first interface, and impurities at this interface will have enhanced absorption. The min R can also be changed through polarization, which allows for the study of the second interface. This manipulation of the light is directed by Equation A-6, which applies to three-phase systems.